Supporting Information

Formic acid dehydrogenation catalysed by a novel amino-di(*N*-heterocyclic carbene) based Ru-CNC pincer complex

Patricia Aufricht, Valeria Nori, Brenda Rabell, Luca Piccirilli, Sakhitha Koranchalil, René W. Larsen, Mathias T. Nielsen* and Martin Nielsen*

Department for Chemistry, Technical University of Denmark (DTU), 2800 Kongens Lyngby, Denmark

General Information

All syntheses, unless otherwise stated, were performed in air. Handling of air-sensitive reagents was conducted under inert gas conditions using standard Schlenk or glovebox techniques. Ligand precursors were commercially achieved and used without further purification. Solvents were deoxygenated by argon bubbling and dried from water impurities by the use of an Inert Puresolv solvent purification system. Ionic liquids were commercially acquired and used without further purification. $RuCl_2(PPh_3)_2(dmf)$ was synthesised according to literature procedure.[1]

Instrumentation

Nuclear Magnetic Resonance spectroscopy (NMR)

NMR spectra were obtained using a Bruker Ascend 400, or 800 MHz spectrometer equipped with BBFO and TCI CryoProbe probes. Chemical shifts are expressed in ppm relative to tetramethylsilane (TMS) for ^{1}H and ^{13}C spectra using residual solvent signal peaks or TMS as internal reference. For ^{31}P spectra, values are expressed in ppm relative to H_3PO_4. Residual solvent chemical shifts are explained according to literature.[2] Coupling constants, if available, are given in Hz as absolute values. Multiplicities are given as singlets (s), doublets (d), triplets (t), heptets (hept), doublets of a doublet of a doublet (ddd) and multiplets (m). Literature-known compounds were analysed only using ^{1}H-NMR spectroscopy to confirm purity. NMR spectra were analysed using MestReNova software.

Single-Crystal X-ray diffraction (SC-XRD)

All crystals were submerged in polybutene oil (Sigma, > 90%) as protection against oxidation and hydrolysis by air. Suitable crystals were identified using light microscopy and harvested

with a MiTeGen cryo loop. They were mounted on a 5-axis goniometer attached to a Rigaku SuperNova dual source CCD-diffractometer. The measurements were conducted at 120 K using either Mo Kα or Cu Kα radiation. Structures were solved using Olex2[3] equipped with SHELXT[4] software using intrinsic phasing and refined to completion using SHELXL employing least square minimizations against F^2. Thermal ellipsoids are printed at 50% probability. All depictions follow the following colour code: hydrogen white, carbon grey, oxygen red, nitrogen blue, chlorine dark green, ruthenium dark blue.

Infrared Spectroscopy (ATR-IR)

Solid-state attenuated total reflectance Fourier transform infrared (ATR-FTIR) spectroscopy was performed employing a VERTEX 80 vacuum Fourier transform spectrometer from Bruker Optics GmbH equipped with a Germanium-coated KBr beam splitter, a LN_2-cooled HgCdTe detector and globar radiation source. The solid samples were brought in contact with a Germanium ATR crystal of a single-reflection ATR accessory from PIKE Technologies, Inc., which in contrast to a conventional diamond ATR crystal is highly transparent in the important spectral region of the Ru-H stretching fundamental transitions around 2000 cm^{-1}. Blocks of 300 co-added scans with a spectral resolution of 2 cm^{-1} were collected both with the sample and of the cleaned ATR crystal before and after sample measurements. Minor traces of residual water vapor absorption were subtracted and gentle corrections for baseline drifts were introduced before the final application of extended ATR corrections compensating for the wavelength-dependent penetration depth of the infrared probe beam into the sample.

High-Resolution Mass Spectrometry (HR-MS)

HR-MS measurements were taken on a Thermo Fisher Orbitrap Exploris 120, mounted with a H-ESI source. All spectra were recorded at 30k FWHM resolution. For analysis of the FADH reactions mixtures: an aliquot was collected (at the first 45 minutes and after 2 cycles and 3 hours, respectively) and dissolved in MeOH/MiliQ water (50:50 v/v) under a N_2 atmosphere, passed through a syringe filter and injected into the HR-MS spectrometer.

Gas chromatography (GC)

GC-TCD measurements were taken on an Agilent Technologies 6890M Network GC system.

Experimental

Synthesis of [$^{i\mathrm{Pr}}$CNC][Cl]$_2$

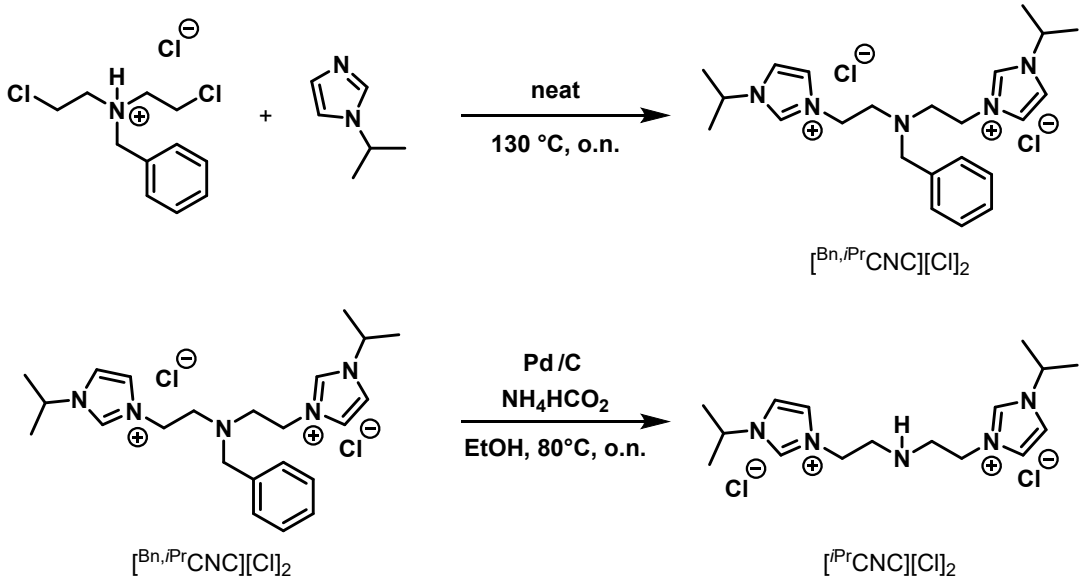

Scheme S1. Two-step proligand synthesis.

Imidazole alkylation: A 250 mL round-bottom flask equipped with a reflux-condenser was charged with a stir bar, *N*-benzyl-bis(2-chloroethyl)amine hydrochloride (6.00 g, 22.34 mmol, 1.00 eq.) and *N*-isopropylimidazole (17.5 g, 158 mmol, 7.10 eq.), before the suspension was stirred at 130°C overnight. In the morning, the reaction mixture was allowed to cool to room temperature. The viscous orange-red solution was washed with Et_2O in portions of 15 mL (stirred with specular), and the milky solution was decanted from the viscous orange material, until the Et_2O fraction ran clear. Enough acetonitrile (MeCN) was added to fully dissolve the viscous material, and the MeCN solution was added to a 600 mL beaker containing 200 mL acetone. The mixture was stirred for approximately 1 hour until a white precipitate was formed. The orange suspension was filtered through a M-coarseness glass frit and the off-white solid was washed with acetone until the filtrate became colourless. The resulting colourless/white powder was dried on the frit for several hours in air, affording [$^{\mathrm{Bn},i\mathrm{Pr}}$CNC][Cl]$_2$ in 88% yield (9.66 g, 19.8 mmol).

^{1}H-NMR (400 MHz, DMSO-d_6) δ (ppm) = 9.38 (d, ^3J = 1.8 Hz, 2H, H_{imi}), 7.87 (t, ^3J = 1.8 Hz, 2H, H_{imi}), 7.70 (t, ^3J = 1.8 Hz, 2H, H_{imi}), 7.25 – 7.18 (broad multiplet, 3H, H_{arom}), 6.98 – 6.92 (broad multiplet, 2H, H_{arom}), 4.64 (hept, ^3J = 6.7 Hz, 2H, C*H*), 4.32 (t, ^3J = 6.3 Hz, 4H, CH_2), 3.64 (s, 2H, CH_2), 2.92 (t, ^3J = 6.3 Hz, 4H, CH_2), 1.47 (d, ^3J = 6.7 Hz, 12H, CH_3).

^{13}C-NMR (101 MHz, DMSO-d_6) δ (ppm) = 138.50, 135.32, 128.16, 128.12, 126.98, 122.85, 120.24, 57.31, 52.55, 52.13, 46.38, 22.43.

HR-MS: m/z: [M−Cl]$^+$ Calc for $C_{23}H_{35}ClN_5$ 416.2576; Found 416.2576, [M−2Cl]$^{2+}$ Calc for $C_{23}H_{35}N_5$ 190.6441; Found 190.6440, [M−2Cl−H]$^+$ Calc for $C_{23}H_{34}N_5$ 380.2809; 380.2809.

Deprotection: [$^{Bn,i Pr}$CNC][Cl]$_2$ (9.60 g, 19.6 mmol, 1.00 eq.) and NH_4HCO_2 (20.0 g, 317 mmol, 16.1 eq.) were added to a 500 mL three-neck round-bottom flask equipped with two glass-stoppers and a reflux-condenser before being dissolved in EtOH (250 mL). The EtOH solution was sparged with argon-gas for 30 minutes before Pd/C (10%) (1.80 g, 15.7 mmol, 0.78 eq.) was added to the reaction mixture under argon counterflow. The suspension was refluxed under an argon-atmosphere overnight. After letting the black mixture cool to room temperature, the suspension was filtered through celite, and the pad was extracted with 2 x 20 mL more EtOH. Solvent was removed *in vacuo* from the combined filtrate to obtain [$^{i Pr}$CNC][Cl]$_2$ as an off-white (later yellow) oil in 90% yield (7.05 g, 17.7 mmol).

^{1}H-NMR (400 MHz, DMSO-d_6) δ (ppm) = 9.61 (s, 2H, H_{imi}), 7.91 (t, ^3J = 1.8 Hz, 2H, H_{imi}), 7.84 (t, ^3J = 1.8 Hz, 2H, H_{imi}), 4.65 (hept, ^3J = 6.7 Hz, 2H, CH), 4.26 (t, ^3J = 5.8 Hz, 4H, CH_2), 2.98 (t, ^3J = 5.8 Hz, 4H, CH_2), 1.48 (d, ^3J = 6.7 Hz, 12H, CH_3).

^{13}C-NMR (101 MHz, DMSO-d_6) δ (ppm) = 135.42, 122.87, 120.16, 52.08, 48.31, 47.35, 22.40.

HR-MS: m/z: $[M-Cl]^+$ Calc for $C_{16}H_{29}ClN_5$ 326.2106; Found 326.2106, $[M-2Cl]^{2+}$ Calc for $C_{16}H_{29}N_5$ 145.6205; Found 145.6206, $[M-2Cl-H]^+$ Calc for $C_{16}H_{28}N_5$ 290.2339; Found 290.2340.

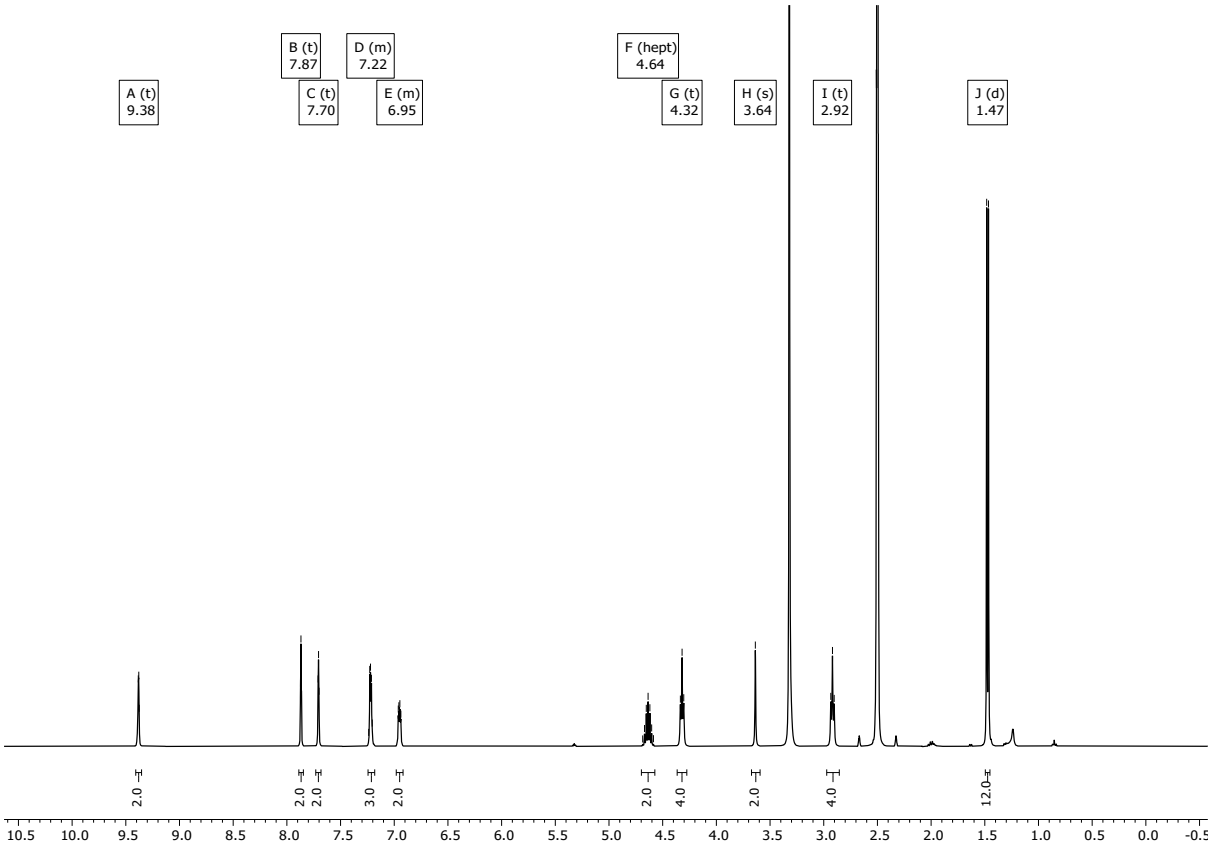

Figure S1. ^{1}H NMR spectrum (400 MHz, DMSO-d_6) of [$^{Bn,i Pr}$CNC][Cl]$_2$.

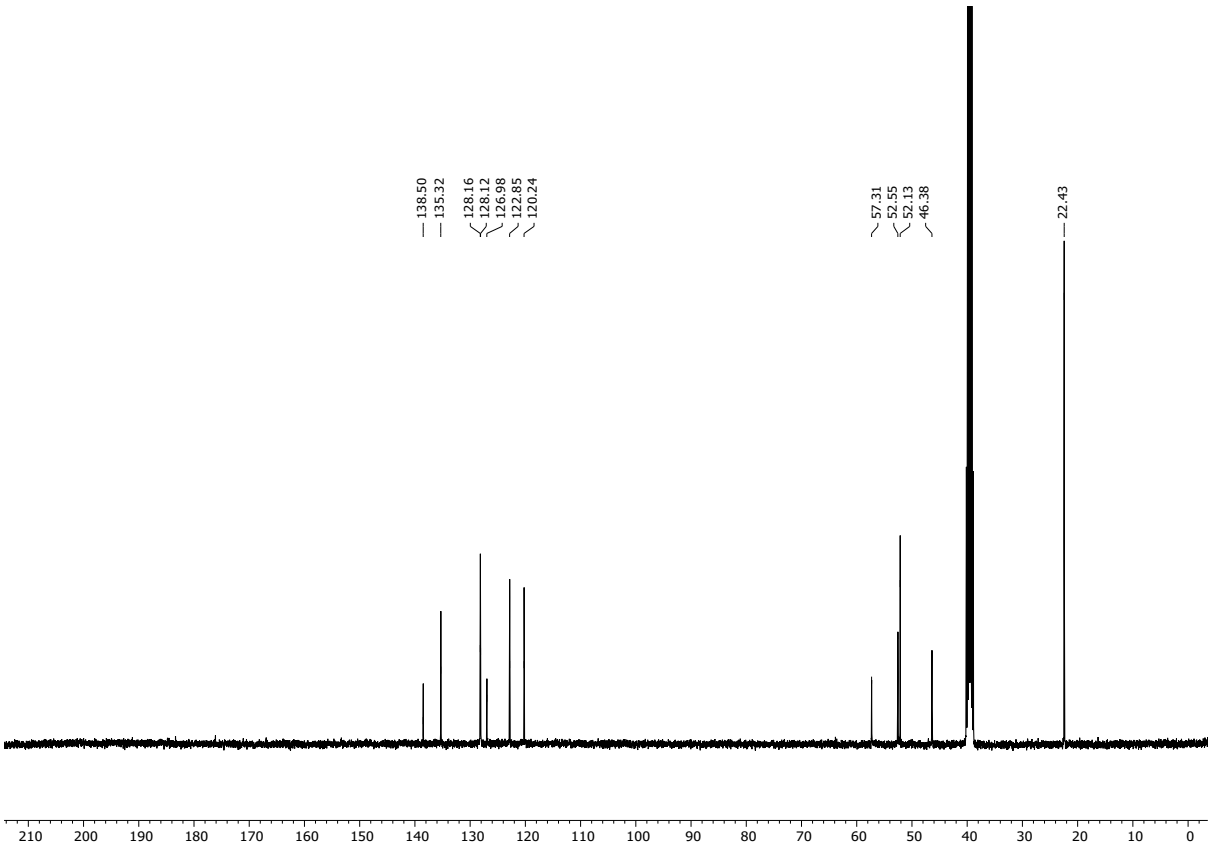

Figure S2. $^{13}C\{^{1}H\}$ NMR spectrum (101 MHz, DMSO-d_6) of $[^{Bn,i\text{Pr}}CNC][Cl]_2$.

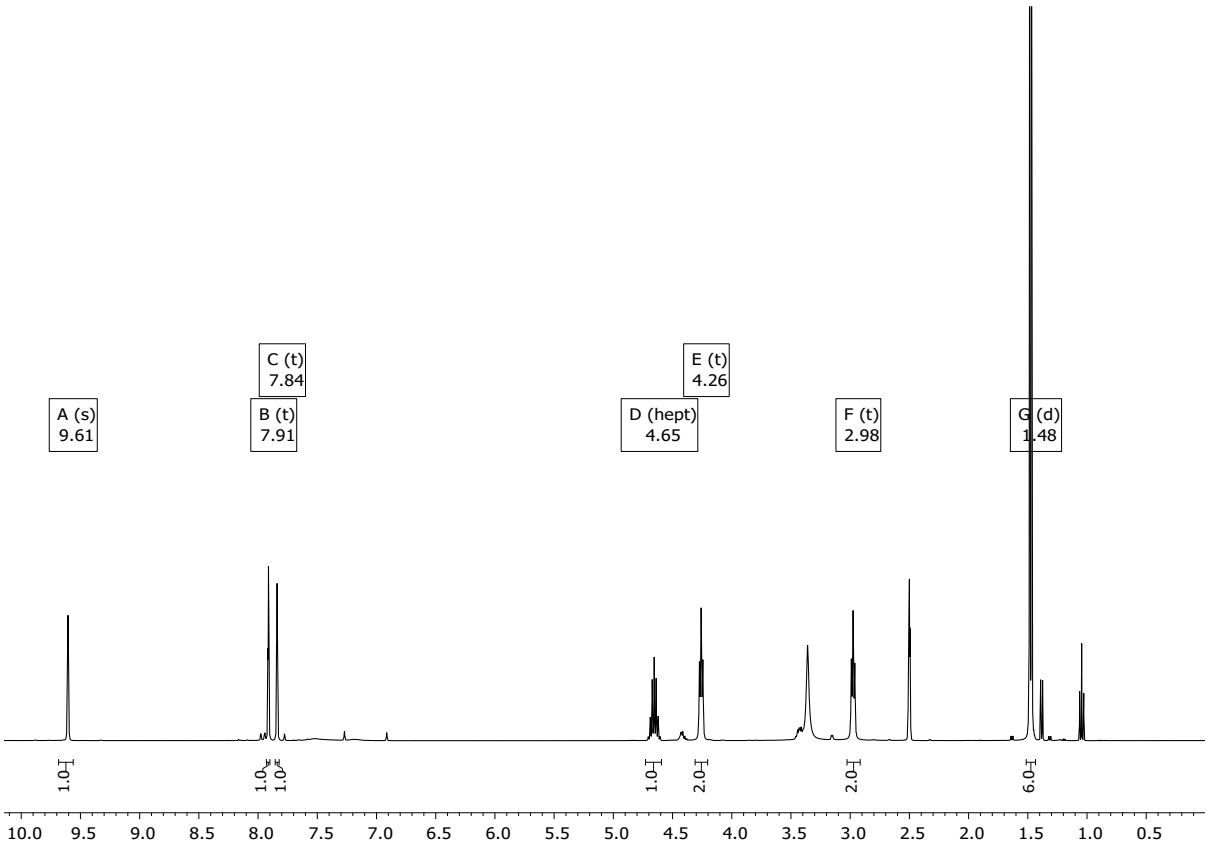

Figure S3. ^{1}H NMR spectrum (400 MHz, DMSO-d_6) of $[^{i\text{Pr}}CNC][Cl]_2$.

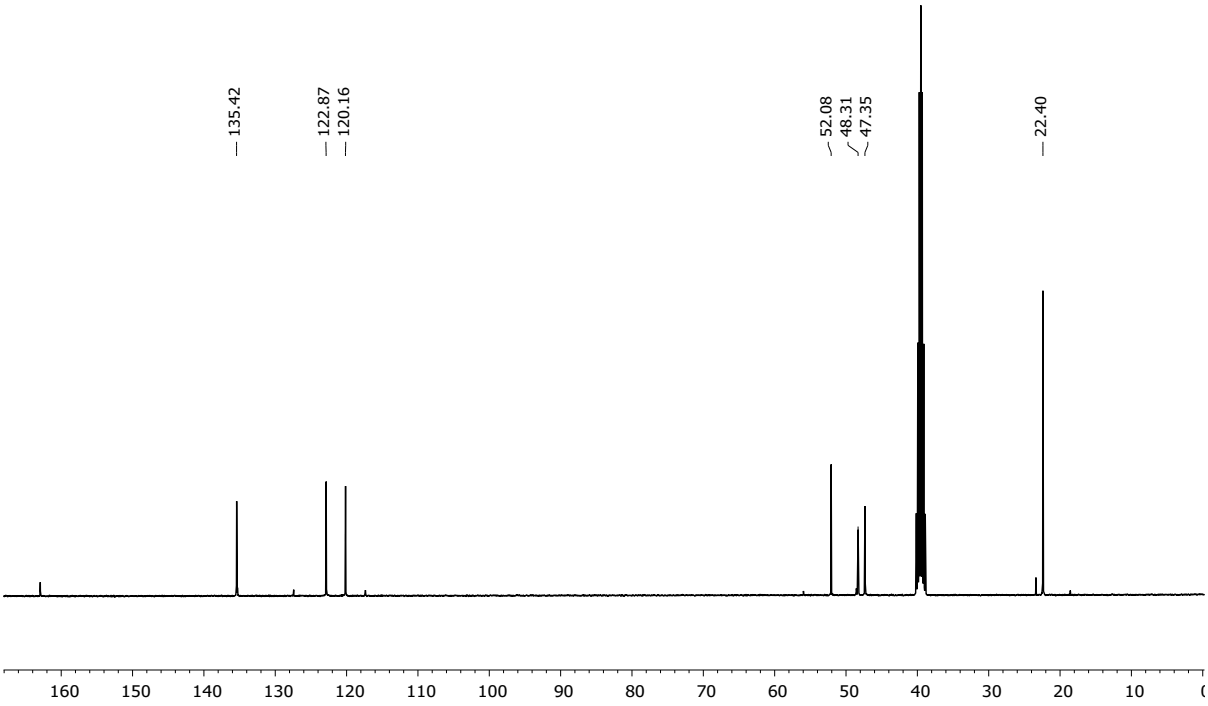

Figure S4. $^{13}C\{^{1}H\}$ NMR spectrum (101 MHz, DMSO-d_6) of [$^{i\text{Pr}}$CNC][Cl]$_2$.

Synthesis of $^{i\text{Pr}}$CNC(AgCl)$_2$

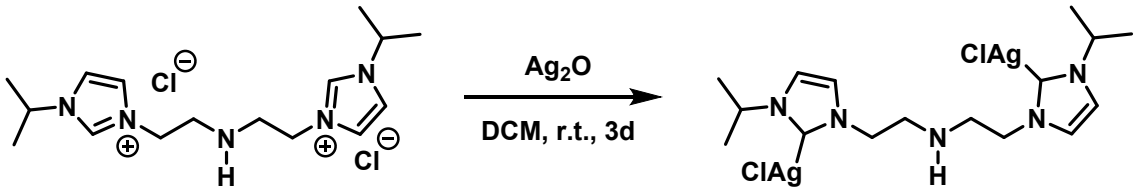

[$^{i\text{Pr}}$CNC][Cl]$_2$ $^{i\text{Pr}}$CNC(AgCl)$_2$

In a 250 mL round-bottom flask charged with a stirbar, [$^{i\text{Pr}}$CNC][Cl]$_2$ (3.76 g, 10.39 mmol, 1.00 eq.) was suspended in DCM (40 mL) and Ag_2O (7.00 g, 30.21 mmol, 2.91 eq.) was added. The reaction flask was covered in aluminium foil and stirred for three days at room temperature. The resulting black suspension was filtered through celite and washed with DCM (15 mL). DCM was removed *in vacuo* affording an off-white foam, that turns metallic, red-brown after exposure to light (within minutes).

^{1}H-NMR (400 MHz, DMSO-d_6) δ (ppm) = 7.54 (d, ^3J = 1.8 Hz, 2H, H_{imi}), 7.44 (d, ^3J = 1.8 Hz, 2H, H_{imi}), 4.64 (hept, ^3J = 6.8 Hz, 2H, C*H*), 4.13 (t, ^3J = 6.0 Hz, 4H, CH_2), 2.91 (q, ^3J = 6.0 Hz, 4H, CH_2), 1.42 (d, ^3J = 6.8 Hz, 12H, CH_3).

^{13}C-NMR (101 MHz, DMSO) δ (ppm) = 177.18 (AgC_{imi}), 122.25 (C_{imi}), 118.15 (C_{imi}), 53.38 (*C*H), 50.99 (*C*H$_2$), 49.61 (*C*H$_2$), 23.36 (*C*H$_3$). (+impurities+ DCM solvent signals).

^{1}H-NMR (400 MHz, 298 K, CD_2Cl_2) δ (ppm) = 7.19 (d, ^3J = 1.8 Hz, 2H, H_{imi}), 7.06 (d, ^3J = 2.0 Hz, 2H, H_{imi}), 4.74 (hept, ^3J = 7.0 Hz, 2H, C*H*), 4.19 (t, ^3J = 6.0 Hz, 4H, CH_2), 3.02 (d, ^3J = 6.1 Hz, 4H, CH_2), 1.46 (d, ^3J = 6.8 Hz, 12H, CH_3).

Unable to establish an appropriate isotopic pattern from HR-MS following decomposition. The decomposition is also observed inside the glovebox.

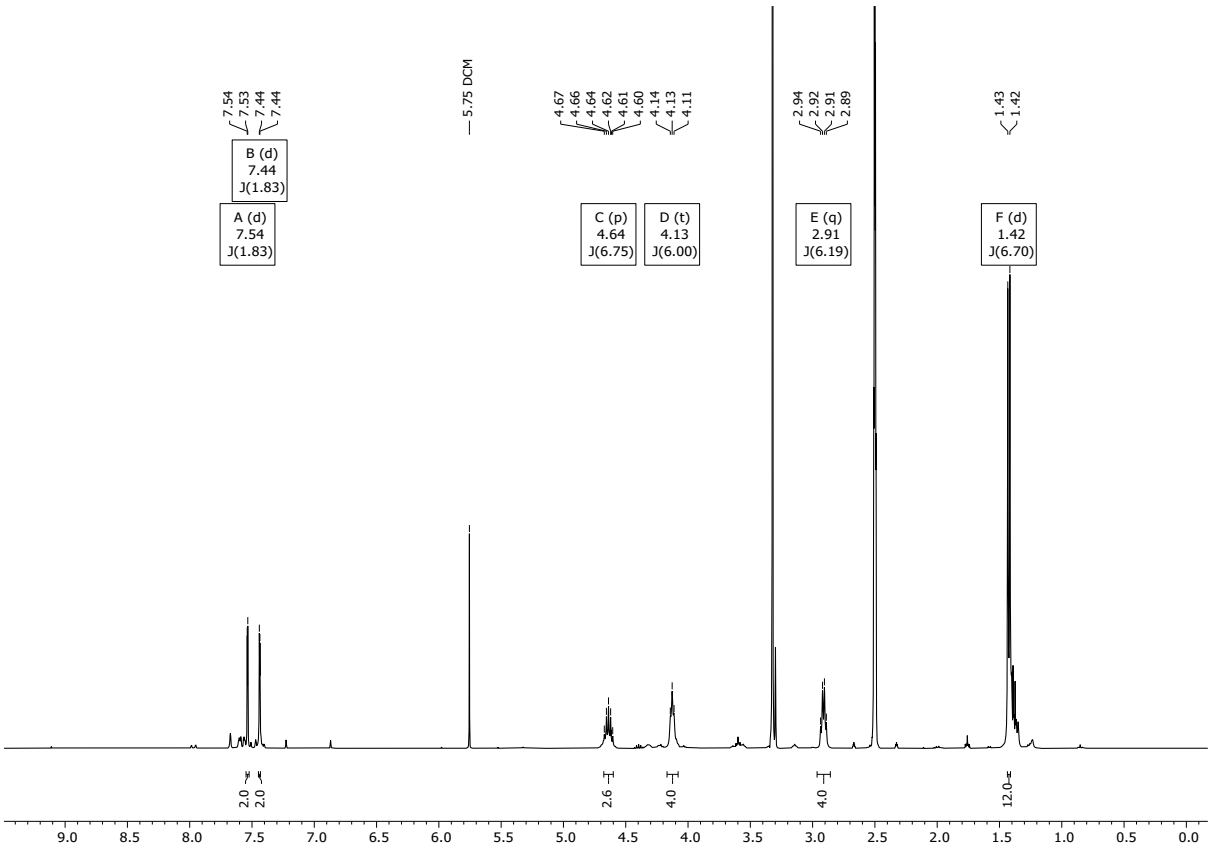

Figure S5. ^{1}H NMR spectrum (400 MHz, DMSO-d_6) of $^{i\text{Pr}}$CNC(AgCl)$_2$.

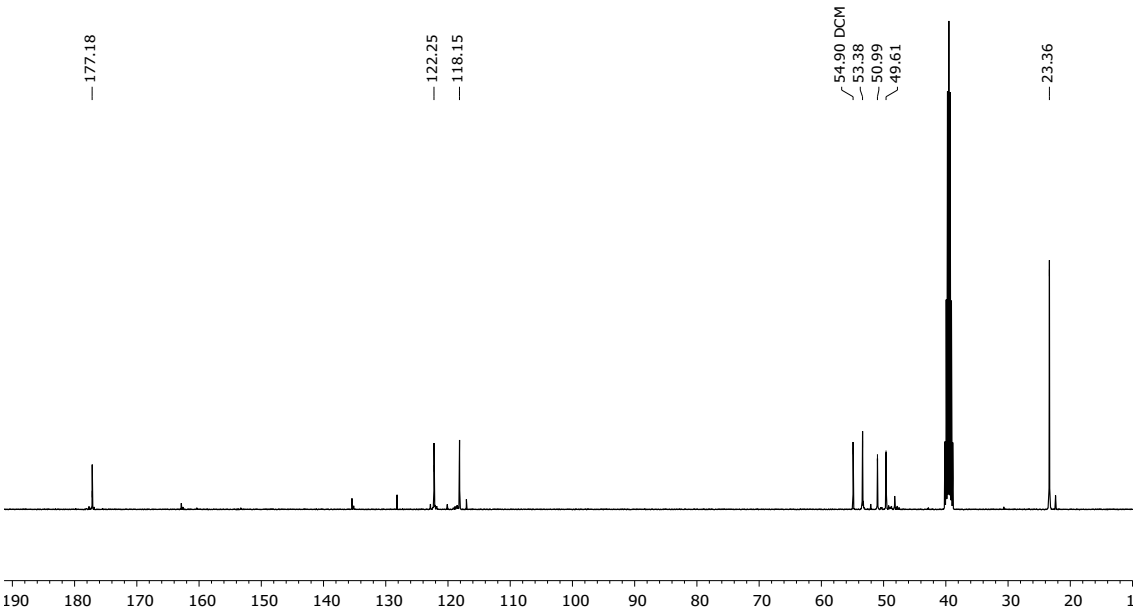

Figure S6. ^{13}C{^{1}H} NMR spectrum (101 MHz, DMSO-d_6) of $^{i\text{Pr}}$CNC(AgCl)$_2$.

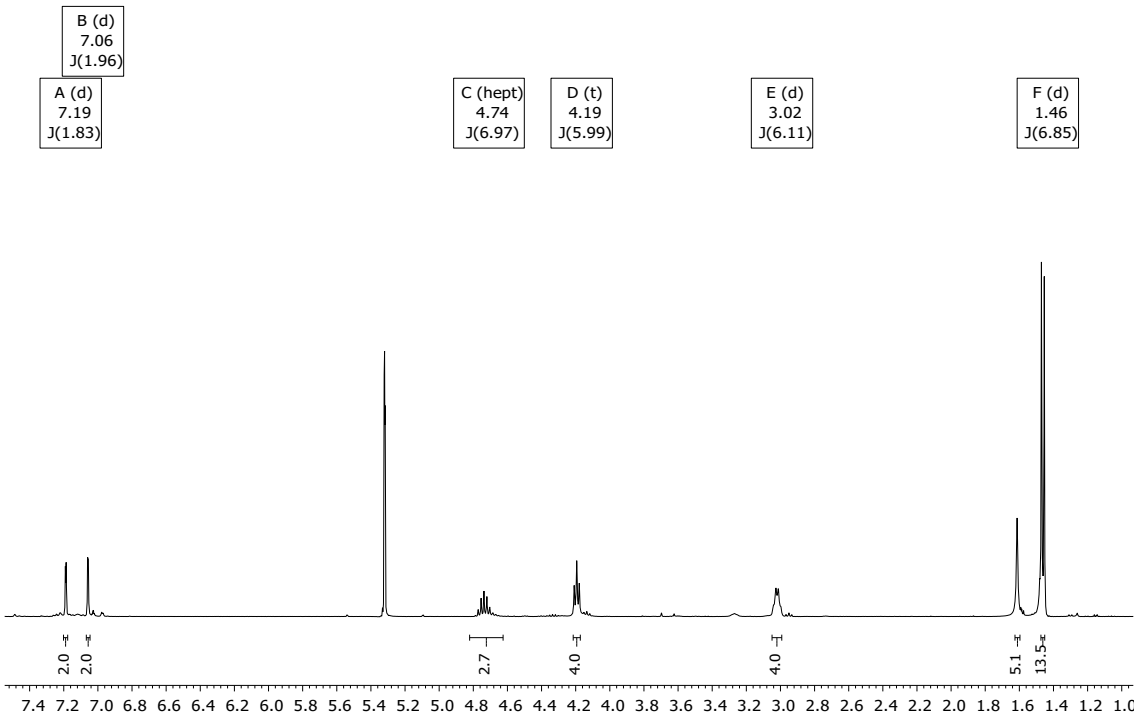

Figure S7. ^{1}H NMR spectrum (400 MHz, CD_2Cl_2) of $^{i\text{Pr}}CNC(AgCl)_2$.

Synthesis of $^{i\text{Pr}}$CNC-Ru(Cl)$_2$CO, Ru-1

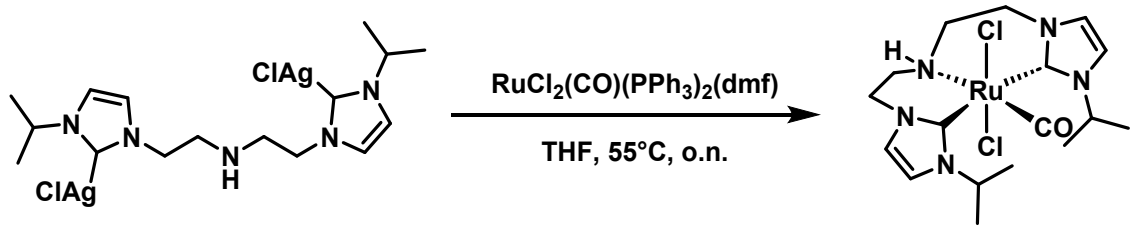

$^{i\text{Pr}}$CNC(AgCl)$_2$ Ru-1

Inside the glovebox, a 50 mL bottom-flatten flask was charge with a stirbar, $^{i\text{Pr}}$CNC(AgCl)$_2$ (150 mg, 260.4 µmol, 1.00 eq.), and $RuCl_2(CO)(PPh_3)_2$(dmf) (203.6 mg, 255.2 µmol, 0.98 eq.). The powders were suspended in dry THF (24 mL) and the flask was placed directly on-top of the stir plate, and the suspension was heated to 55 °C for up to 48 hours under vigorous stirring. The stirring was stopped, allowing the solids the solids were allowed to settle at the bottom, before the solution was passed through a Whatman glass filter fitted inside a glass Pasteur pipette (23 cm), affording a yellow filtrate that was collected in a 24 mL scintillation vial. Inside the glovebox all volatiles were removed *in vacuo*, the resulting yellowish solid was then brought outside of the glovebox, and the material was finally dissolved in MeOH (16 mL), which immediately causes most PPh_3 to precipitate out. The methanolic solution was collected *via* filtration and then concentrated to about 1 mL *in vacuo*, and the vial was then placed inside the refrigerator for 30 minutes before the dark supernatant was decanted off. The bright yellow crystals/powder was washed thrice more with cold MeOH (0 ºC, 3 x 0.3 mL), or until the liquid no longer had a dark discolouring to it, and the powder was finally washed thrice with dry Et_2O (3 x 20 mL). The yellow powder was dissolved in as little volume MeOH possible, passed through a Whatman glass filter, concentrated to no more than a mililiter *in vacuo*, precipitated with enough Et_2O, and the liquid was removed before the solid was placed to dry *in vacuo* for a couple of hours affording **Ru-1** in up-to 38% yield (48.3 mg, 99 µmol). Crystals suitable for single-crystal X-ray diffraction were obtained from either 1) layering of Et_2O into a concentrated THF solution of **Ru-1** or 2) from slow solvent evaporation from a concentration methanolic solution of **Ru-1**.

^{1}H-NMR (800 MHz, CD_3CN) δ (ppm) = 7.18 (d, ^3J = 1.9 Hz, 2H, H_{imi}), 7.10 (d, ^3J = 1.9 Hz, 2H, H_{imi}), 5.49 (hept, ^3J = 6.8 Hz, 2H, C*H*),4.86 (ddd, ^3J = 14.1, 8.5, 3.5 Hz, 2H, CH_2), 4.22 (ddd, ^3J = 14.1, 5.8, 3.5 Hz, 2H, CH_2), 4.07 (s, 1H, N*H*), 3.42 – 3.33 (m, 2H, CH_2), 3.03 – 2.97 (m, 2H, CH_2), 1.50 (d, ^3J = 6.8 Hz, 6H, CH_3), 1.47 (d, ^3J = 6.8 Hz, 6H, CH_3).

^{13}C NMR (201 MHz, CD_3CN) δ (ppm) = 208.78 (Ru-**C**O), 183.97 (Ru-**C**(NHC)), 123.63 (C_{imi}), 117.54 (C_{imi}), 51.99 (CH_2), 51.97 (*C*H), 48.63 (CH_2), 24.50 (CH_3), 24.28 (CH_3).

HR-MS: m/z: $[M-Cl]^+$ Calc for $RuON_5ClC_{17}H_{27}$ 454.0942, Found 454.0942.

A biproduct that we sometime observe from this reaction is $[AgClPPh_3]_4$ as white crystals, that was removed *via* mechanical separation as this compound shares similar solubility properties as **Ru-1**. The yellow powder was recrystallized from a concentrated MeOH solution at −18°C. When small colourless crystals formed alongside the desired long yellow needles, as seen in below image, the two types of crystals were separated by mechanical sieving.

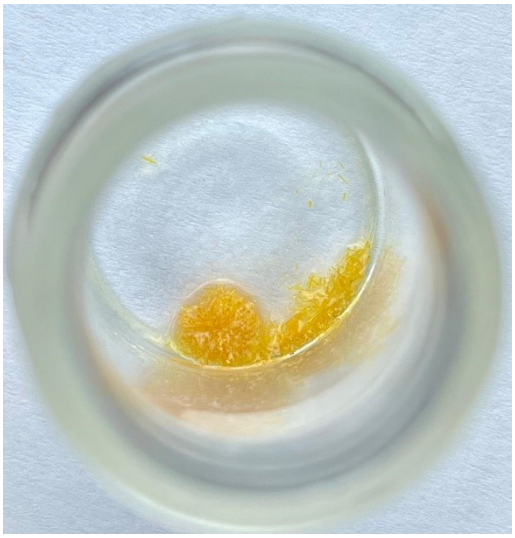

The IR spectrum of **Ru-1** features a medium-intensity and a strong-intensity absorption band attributed to the characteristic stretching frequencies of the amino (3129 cm^{-1}) and carbonyl (1915 cm^{-1}) functional groups, respectively (**Figure S8**). No absorption resonance at 1639 cm^{-1} relating to the precursor was detected.[1]

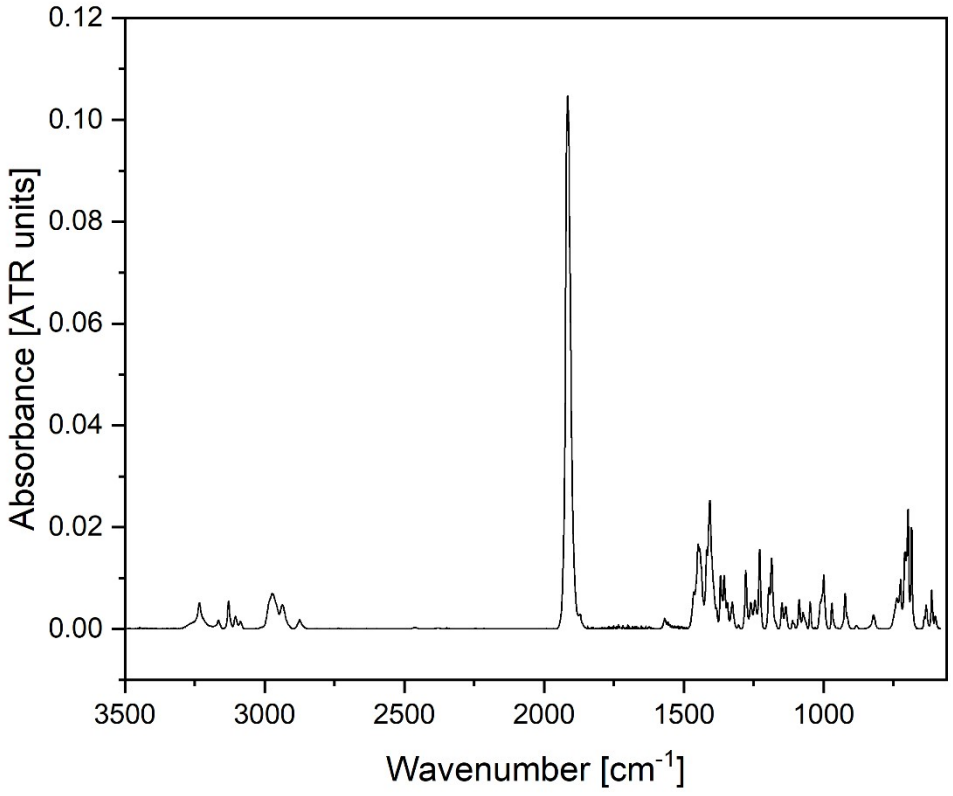

Figure S8. FTIR spectrum of **Ru-1**.

Wavenumber / cm^{-1}	**Absolute Intensity / A.U**
3233	0,005
3164	0,002
3129	0,005
3104	0,003
3087	0,001

2974	0,007
2936	0,005
2875	0,002
1915 (CO)	0,105
1569	0,002
1449	0,017
1407	0,025
1369	0,011
1356	0,011
1327	0,005
1278	0,012
1260	0,005
1246	0,006
1229	0,016
1186	0,014
1149	0,005
1136	0,004
1111	0,002
1087	0,006
1074	0,003
1048	0,005
999	0,011
970	0,005
923	0,007
882	0,001
822	0,003
725	0,01
697	0,024
685	0,02
633	0,005
613	0,008

The aromatic region features two characteristic narrow doublets (J ~ 2 Hz), signals A and B, corresponding to the C4 and C5 of the imidazole-2-ylidene moieties. The *i*Pr wingtips give rise to three distinctive signals, namely signals C (heptet), I (doublet), and J (doublet), owing to the methine and two chemically inequivalent methyl groups, respectively. From the {^{1}H-^{1}H} COSY NMR spectrum (**Figure S10**) we establish that the remaining signals, D (ddd), E (ddd), G (m), and H (m) can be attributed to the ethyl linkers and the broad signal F (s), lacking any fine structure, is consistent with the amino proton. Moreover, because of the absence of off-diagonal elements in the COSY spectrum with signal F, we can assign signals D and E to the diastereotopic methylene protons adjacent to the NHC-moiety. Signals G and H, on the other hand, feature this cross-peak, and can thus be assigned to the methylene protons adjacent to the amino group and help explain the complex multiplicity observed in **Figure S9**. Importantly, no residual triphenylphosphine is observed (**Figure S14**).

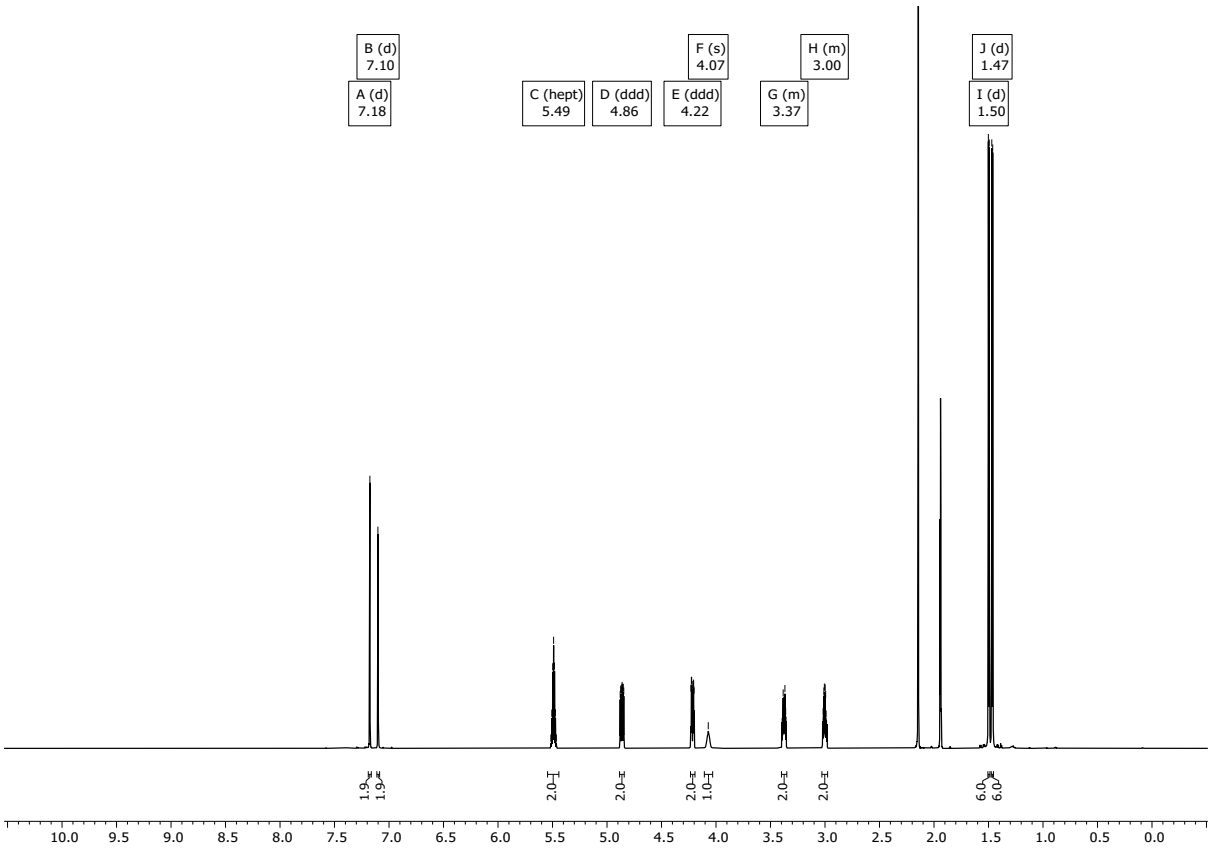

Figure S9. ^{1}H NMR spectrum (800 MHz, CD_3CN) of **Ru-1**.

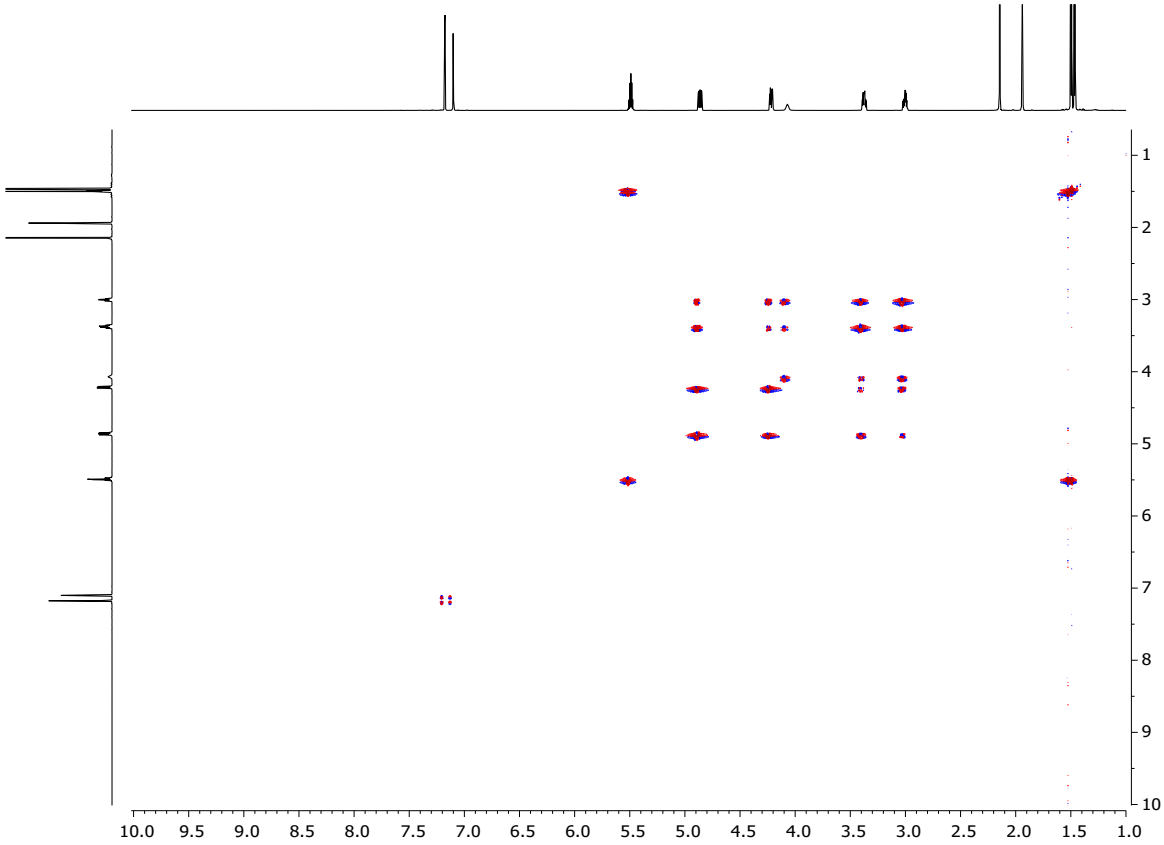

Figure S10. {^{1}H-^{1}H} COSY NMR spectrum (800 MHz, CD_3CN) of **Ru-1**.

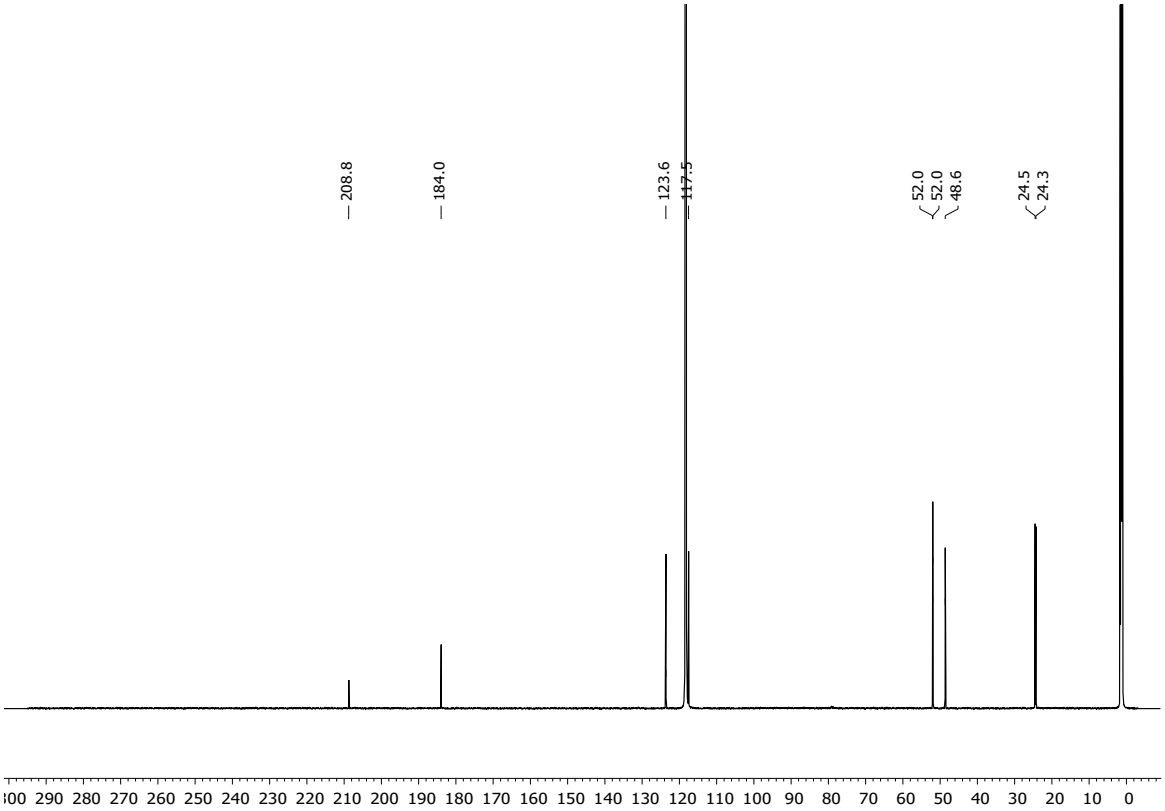

Figure S11. $^{13}C\{^{1}H\}$ NMR spectrum (201 MHz, CD_3CN) of **Ru-1**.

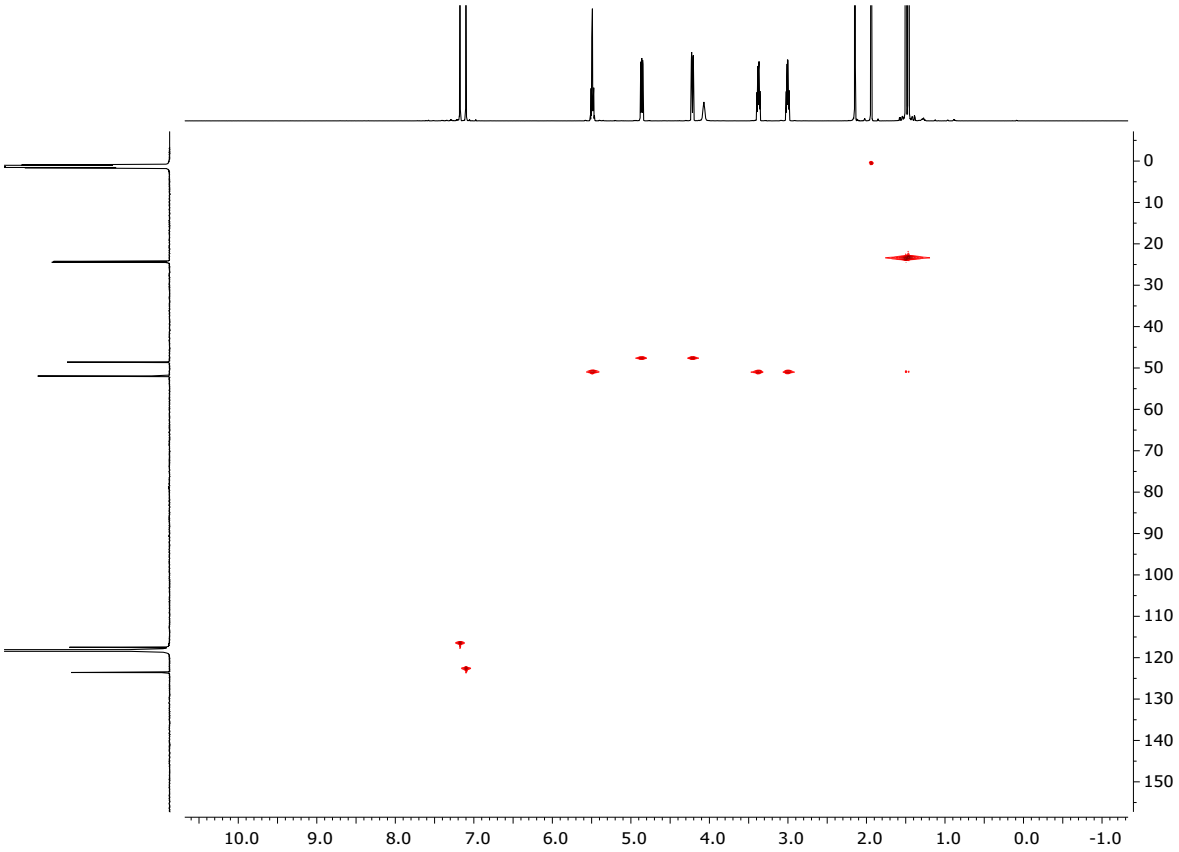

Figure S12. $\{^{1}H\text{-}^{13}C\}$ HSQC NMR spectrum (800 MHz, CD_3CN) of **Ru-1**.

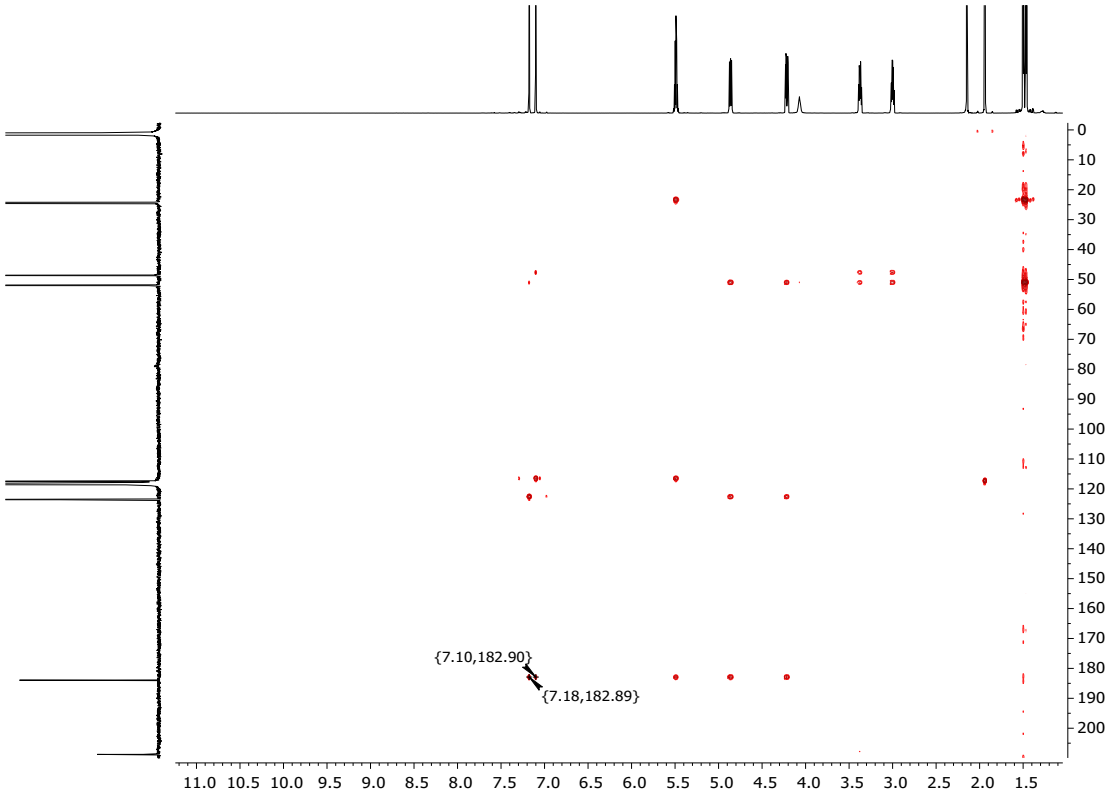

Figure S13 {^{1}H-^{13}C} HMBC NMR spectrum (800 MHz, CD_3CN) of **Ru-1**.

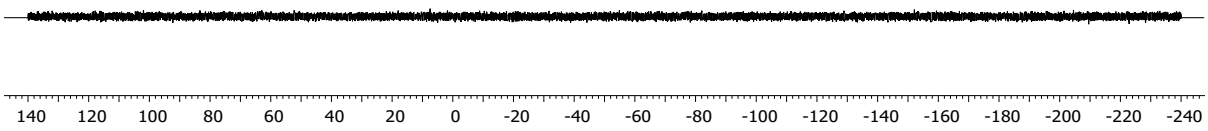

Figure S14. ^{31}P{^{1}H} NMR spectrum (162 MHz, CD_3CN) of **Ru-1**

The bonding metrics of the imidazole-2-ylidine moieties, *e.g.*, the N-C(NHC)-N and C=C bond lengths, are consistent with those observed in other NHC-bearing complexes, see **Tables S2 to S4**.[18–22]

Table S1. Crystallographic data for **Ru-1**.

	Ru-1
Empirical formula	$C_{17}H_{27}Cl_2N_5ORu$
Formula weight (g/mol)	489.40
Temperature (K)	119.99(18)
Crystal system	monoclinic
Space group	$P2_1/c$
a (Å)	10.1376(2)
b (Å)	15.2198(2)
c (Å)	13.6429(2)
α (deg)	90
β (deg)	93.669(10)
γ (deg)	90
Volume (Å^3)	2100.68(6)
Z	4
ρ_{calc} (g/cm^3)	1.547
μ (mm^{-1})	8.511
F(000)	1000.0
Crystal size / mm^3	0.029 × 0.019 × 0.017
Radiation	Cu Kα (λ = 1.54184)
2Θ range for data collection (deg)	8.714 to 140.098
Index ranges	-12 ≤ h ≤ 12, -18 ≤ k ≤ 18, -16 ≤ l ≤ 16
Reflections collected	41312
Independent reflections	3994 [R_{int} = 0.0769, R_{sigma} = 0.0296]
Data/restraints/parameters	3994/0/239
Goodness-of-fit on F^2	1.041
Final R indexes [I>=2σ (I)]	R_1 = 0.0340, wR_2 = 0.0861
Final R indexes [all data]	R_1 = 0.0379, wR_2 = 0.0882
Largest diff. peak/hole / e Å^{-3}	1.67/-0.95

Table S2. Bond Lengths from crystallographic data for **Ru-1**.

Atom	**Atom**	**Length/Å**	**Atom**	**Atom**	**Length/Å**
Ru01	Cl02	2.4188(7)	O007	C00L	1.149(5)

Ru01	Cl03	2.4319(7)	N008	C009	1.357(4)
Ru01	C009	2.096(3)	N008	C00G	1.474(4)
Ru01	C00A	2.105(3)	N008	C00M	1.389(4)
Ru01	N00C	2.247(3)	C00B	C00E	1.344(4)
Ru01	C00L	1.817(4)	N00C	C00F	1.459(4)
N004	C00A	1.359(4)	N00C	C00I	1.468(4)
N004	C00B	1.383(4)	C00D	C00N	1.514(4)
N004	C00J	1.457(4)	C00D	C00Q	1.530(4)
N005	C00A	1.362(4)	C00F	C00J	1.507(4)
N005	C00D	1.479(4)	C00G	C00O	1.524(4)
N005	C00E	1.387(4)	C00G	C00P	1.520(4)
N006	C009	1.361(4)	C00H	C00I	1.510(4)
N006	C00H	1.460(4)	C00K	C00M	1.331(5)
N006	C00K	1.382(4)			

Table S3. Bond Angles.

Atom	**Atom**	**Atom**	**Angle/˚**	**Atom**	**Atom**	**Atom**	**Angle/˚**
Cl02	Ru01	Cl03	175.35(3)	C00M	N008	C00G	123.1(3)
C009	Ru01	Cl02	89.13(8)	N006	C009	Ru01	122.9(2)
C009	Ru01	Cl03	92.49(8)	N008	C009	Ru01	132.9(2)
C009	Ru01	C00A	173.21(11)	N008	C009	N006	104.1(3)
C009	Ru01	N00C	84.03(11)	N004	C00A	Ru01	123.1(2)
C00A	Ru01	Cl02	91.59(8)	N004	C00A	N005	103.9(2)
C00A	Ru01	Cl03	86.30(8)	N005	C00A	Ru01	133.0(2)
C00A	Ru01	N00C	89.38(11)	C00E	C00B	N004	106.8(3)
N00C	Ru01	Cl02	81.77(10)	C00F	N00C	Ru01	118.4(2)
N00C	Ru01	Cl03	94.06(10)	C00F	N00C	C00I	112.1(3)
C00L	Ru01	Cl02	93.56(11)	C00I	N00C	Ru01	120.6(2)

Atom	Atom	Atom	Angle/˚	Atom	Atom	Atom	Angle/˚
C00L	Ru01	Cl03	90.75(11)	N005	C00D	C00N	109.6(3)
C00L	Ru01	C009	91.58(13)	N005	C00D	C00Q	110.4(3)
C00L	Ru01	C00A	95.12(12)	C00N	C00D	C00Q	112.0(3)
C00L	Ru01	N00C	173.62(14)	C00B	C00E	N005	106.7(2)
C00A	N004	C00B	111.4(2)	N00C	C00F	C00J	111.3(2)
C00A	N004	C00J	125.3(2)	N008	C00G	C00O	109.9(3)
C00B	N004	C00J	123.2(2)	N008	C00G	C00P	110.6(3)
C00A	N005	C00D	126.4(2)	C00P	C00G	C00O	112.3(3)
C00A	N005	C00E	111.2(2)	N006	C00H	C00I	112.4(2)
C00E	N005	C00D	122.4(2)	N00C	C00I	C00H	116.5(3)
C009	N006	C00H	123.5(2)	N004	C00J	C00F	113.0(2)
C009	N006	C00K	111.3(3)	C00M	C00K	N006	106.5(3)
C00K	N006	C00H	124.9(3)	O007	C00L	Ru01	177.5(3)
C009	N008	C00G	126.1(3)	C00K	C00M	N008	107.6(3)
C009	N008	C00M	110.4(3)				

Table S4. Torsion Angles.

A	B	C	D	Angle/˚	A	B	C	D	Angle/˚
Ru01	N00C	C00F	C00J	-47.1(3)	C00E	N005	C00A	Ru01	-179.4(2)
Ru01	N00C	C00I	C00H	-12.7(4)	C00E	N005	C00A	N004	1.4(3)
N004	C00B	C00E	N005	0.5(3)	C00E	N005	C00D	C00N	73.8(4)
N006	C00H	C00I	N00C	61.0(4)	C00E	N005	C00D	C00Q	-50.0(4)
N006	C00K	C00M	N008	0.0(4)	C00F	N00C	C00I	C00H	134.1(3)
C009	N006	C00H	C00I	-52.2(4)	C00G	N008	C009	Ru01	10.7(4)
C009	N006	C00K	C00M	0.8(4)	C00G	N008	C009	N006	-171.8(3)
C009	N008	C00G	C00O	110.3(3)	C00G	N008	C00M	C00K	172.5(3)
C009	N008	C00G	C00P	-125.3(3)	C00H	N006	C009	Ru01	-9.1(4)

A	B	C	D	Angle/˚	A	B	C	D	Angle/˚
C009	N008	C00M	C00K	-0.8(4)	C00H	N006	C009	N008	173.1(3)
C00A	N004	C00B	C00E	0.4(3)	C00H	N006	C00K	C00M	-173.5(3)
C00A	N004	C00J	C00F	-50.2(4)	C00I	N00C	C00F	C00J	165.2(3)
C00A	N005	C00D	C00N	-106.8(3)	C00J	N004	C00A	Ru01	-2.5(4)
C00A	N005	C00D	C00Q	129.4(3)	C00J	N004	C00A	N005	176.8(2)
C00A	N005	C00E	C00B	-1.3(3)	C00J	N004	C00B	C00E	-177.5(3)
C00B	N004	C00A	Ru01	179.64(19)	C00K	N006	C009	Ru01	176.5(2)
C00B	N004	C00A	N005	-1.1(3)	C00K	N006	C009	N008	-1.3(3)
C00B	N004	C00J	C00F	127.4(3)	C00K	N006	C00H	C00I	121.4(3)
N00C	C00F	C00J	N004	75.9(3)	C00M	N008	C009	Ru01	-176.2(2)
C00D	N005	C00A	Ru01	1.1(4)	C00M	N008	C009	N006	1.3(3)
C00D	N005	C00A	N004	-178.0(2)	C00M	N008	C00G	C00O	-62.0(4)
C00D	N005	C00E	C00B	178.2(2)	C00M	N008	C00G	C00P	62.5(4)

FADH Catalysis

General procedure for FADH

A three-neck round-bottom flask (25 or 50 mL) equipped with a cross-shaped magnetic stir bar, a reflux-condenser on the middle neck, a rubber septum on one side and a tube connected to a bubbler on the other side, was flushed with argon via the condenser. The gas flow through the flask was adjusted to a constant low flow. Once ready, the rubber septum was briefly removed to charge the flask with the desired amount of catalyst (0.025, 0.05 or 0.1 mol%) and 1 mL of the desired IL. The mixture was stirred in an oil bath at the chosen temperature (80, 90, 100 °C) under continuous stirring (400 rpm) until complete solubilisation of the catalyst was achieved (3-6 minutes). Then, FA (typically 0.5 mL) was slowly added through the rubber septum and the starting time was recorded. For monitoring the FA consumption, samples of the reaction mixture were taken at different time points (typically 15, 30, 35, 60, 90, 120, 180 min), by inserting the tip of a glass pipette into the reaction mixture and then flushing the sample into an NMR tube with deuterated DMSO. The samples were analysed via ^{1}H-NMR analysis. The imidazolium proton signals (at 7.00 and 7.77 ppm) of the IL were used as internal reference.

Procedure for FADH cycles

The first FADH cycle was performed as described in the general procedure. After the cycle was completed (indicated by the absence of FA in the NMR spectrum of the last sample), the reaction flask was continued to be stirred at the same temperature and under a constant low argon flow until the next cycle was started the following day(s). For initiating the next cycle,

the desired amount of FA was added and the starting time was recorded. Samples were taken at various time points to monitor the FA consumption, following the same procedure as in the first cycle. The same methodology was applied to all subsequent cycles.

TON/TOF calculation

The turnover numbers were calculated using the following formula:

$$TON = \frac{n\,(FA)_{Start}}{n\,(catalyst)} \times conversion$$

The turnover frequencies were calculated using the following formula:

$$TOF = \frac{n\,(FA)_{Start}}{n\,(catalyst)} \times conversion \times \frac{1}{t\,[h]}$$

For the time of TOF_{max}, the timeframe was chosen in which the conversion per unit time was highest (i.e., where the conversion/timeline was the steepest).

Table S5. Control experiment. FA over time in EMIM $PO_2(OEt)_2$ at 90 °C.

Entry	Time	Conv. [%][b]
1	0 min[c]	1
2	10 min	2
3	3 h	2

[a]Reaction conditions: EMIM $PO_2(OEt)_2$ (1 mL), FA (13.3 mmol, 0.5 mL), 90 °C, under gentle flow of nitrogen. NMR error margin of 10%. [b]Determined by ^{1}H-NMR. [c]Sampled before heating, after mixing FA and the IL.

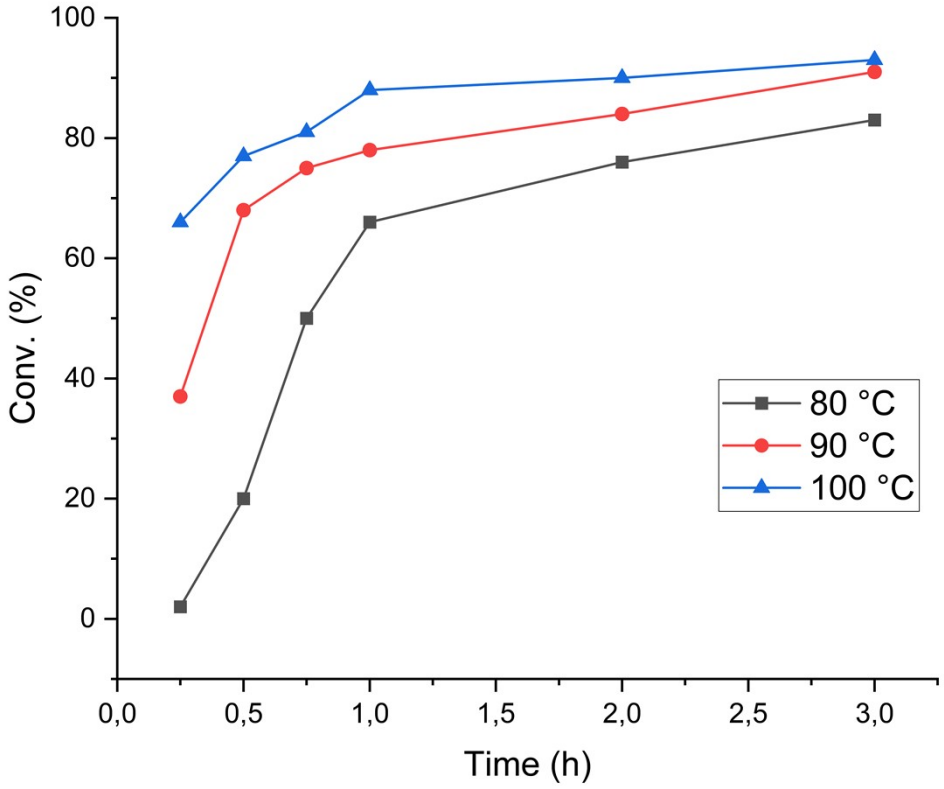

Figure S15. FA conversion *vs* time in EMIM OAc using 0.1 mol% **Ru-1** and 0.5 mL FA at different temperatures (80 °C, 90 °C, 100 °C).

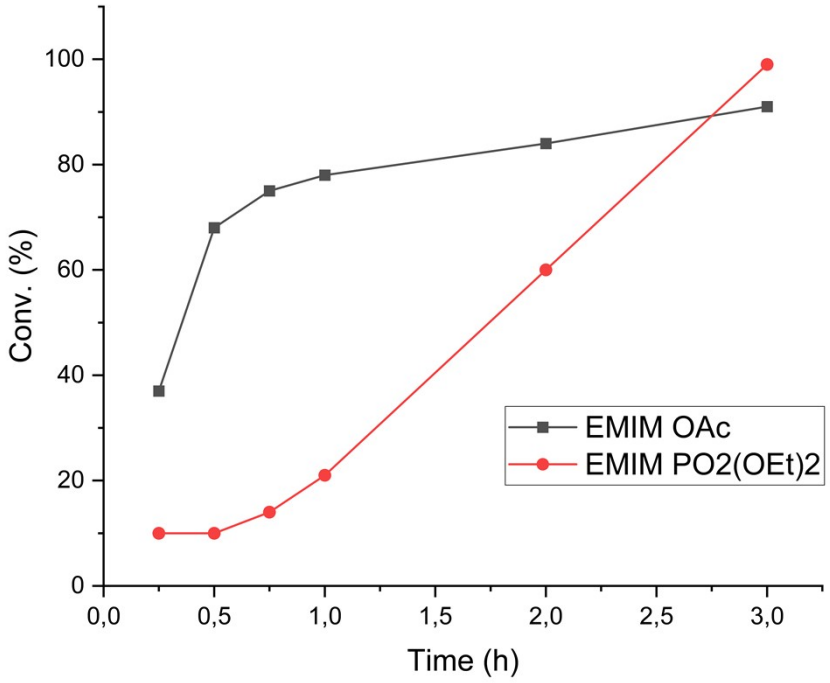

Figure S16. FA conversion *vs* time comparing EMIM OAc *vs* EMIM $PO_2(OEt)_2$ using 0.1 mol% **Ru-1** and 0.5 mL FA, at 90 ºC.

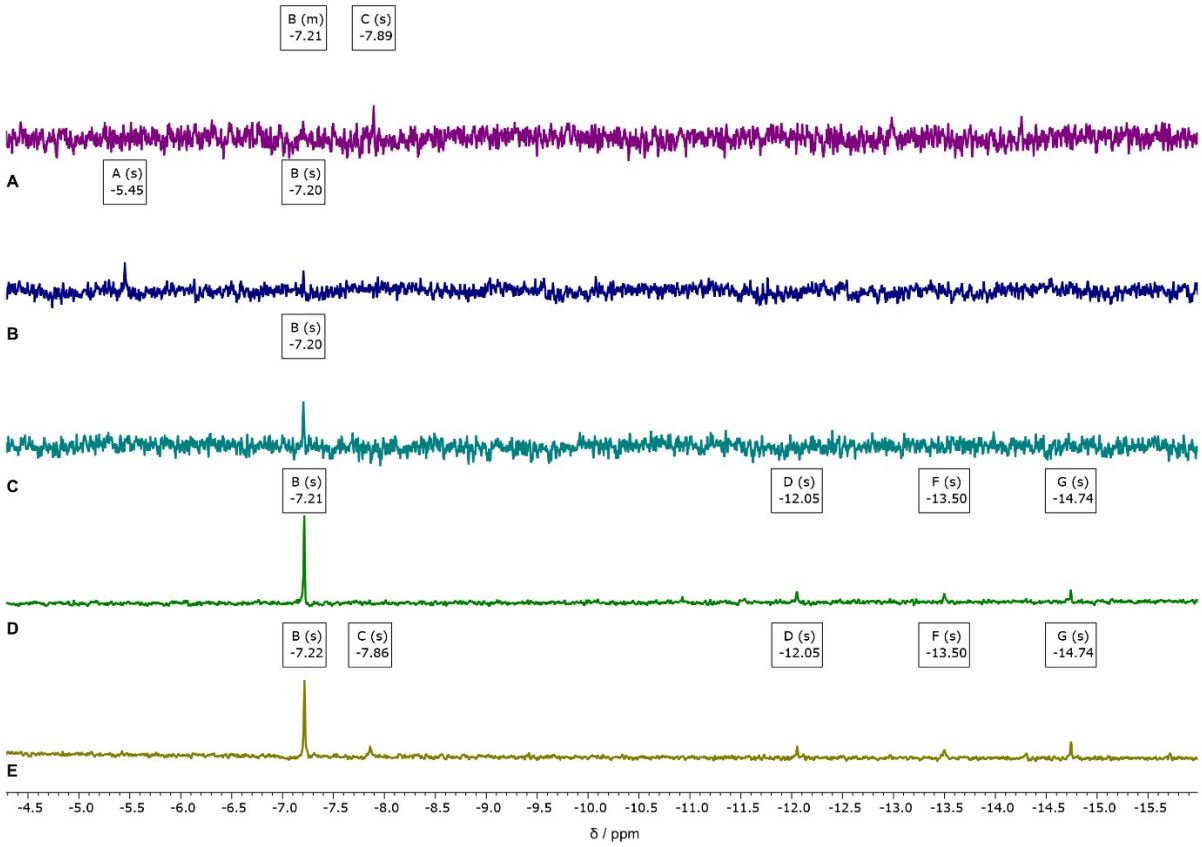

Figure S17. Stacked *in situ* ^{1}H NMR spectra during and post FADH, showing the hydride region. Reaction conditions for **A**: EMIM $PO_2(OEt)_2$ (1 mL), **Ru-1** (0.1 mol%), FA (0.5 mL), 90 °C, cycle 2, 3 h; **B:** EMIM $PO_2(OEt)_2$ (1 mL), **Ru-1** (0.1 mol%), FA (0.5 mL), 90 °C, cycle 5, 3 h; **C:** EMIM $PO_2(OEt)_2$ (1 mL), **Ru-1** (0.1 mol%), FA (0.5 mL), 100 °C, 3 h; **D:** EMIM OAc (1 mL), **Ru-1** (0.05 mol%), FA (0.5 mL), 90 °C, 3 h; **E:** EMIM OAc (1 mL), **Ru-1** (0.1 mol%), FA (0.5 mL), 100 °C, 1 h.

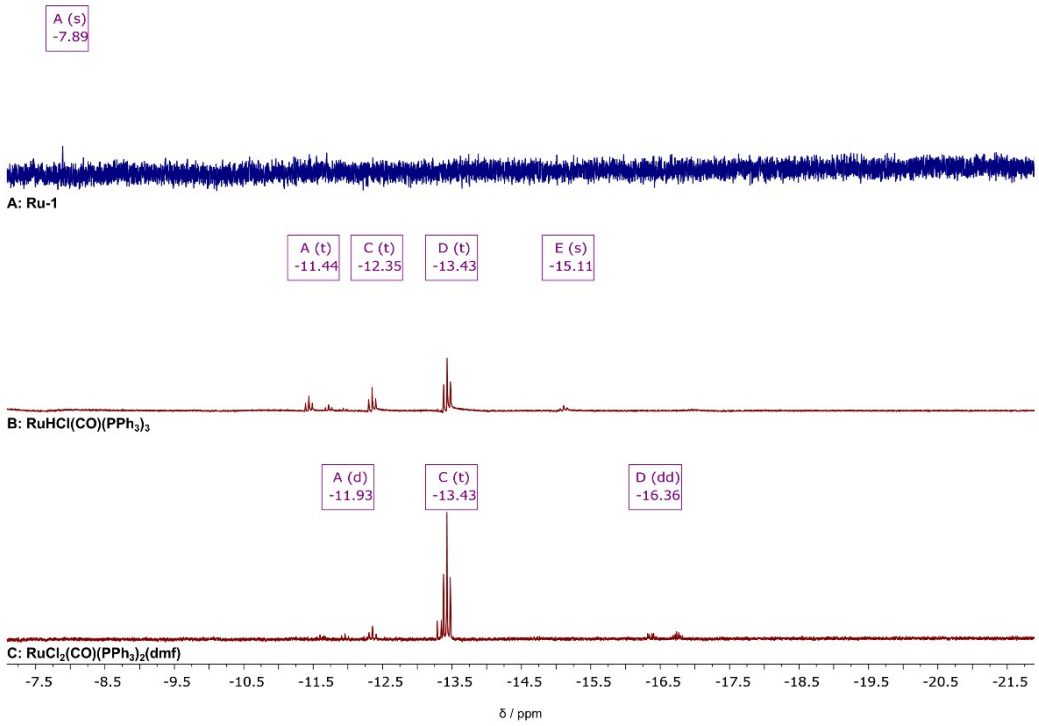

Figure S18a. Stacked *in situ* ^{1}H NMR spectra after 45 minutes of the first cycle of the FADH, showing the hydride region. Reaction conditions for **A**: EMIM $PO_2(OEt)_2$ (1 mL), **Ru-1** (0.1 mol%), FA (0.5 mL), 90 °C, cycle 1, 45 minutes; **B:** EMIM $PO_2(OEt)_2$ (1 mL), **RuHCl(CO)(PPh$_3$)$_3$** (0.1 mol%), FA (0.5 mL), 90 °C, cycle 1, 45 minutes; **C:** EMIM $PO_2(OEt)_2$ (1 mL), **RuCl$_2$(CO)(PPh$_3$)$_2$(dmf)** (0.1 mol%), FA (0.5 mL), 90 °C, cycle 1, 45 minutes.

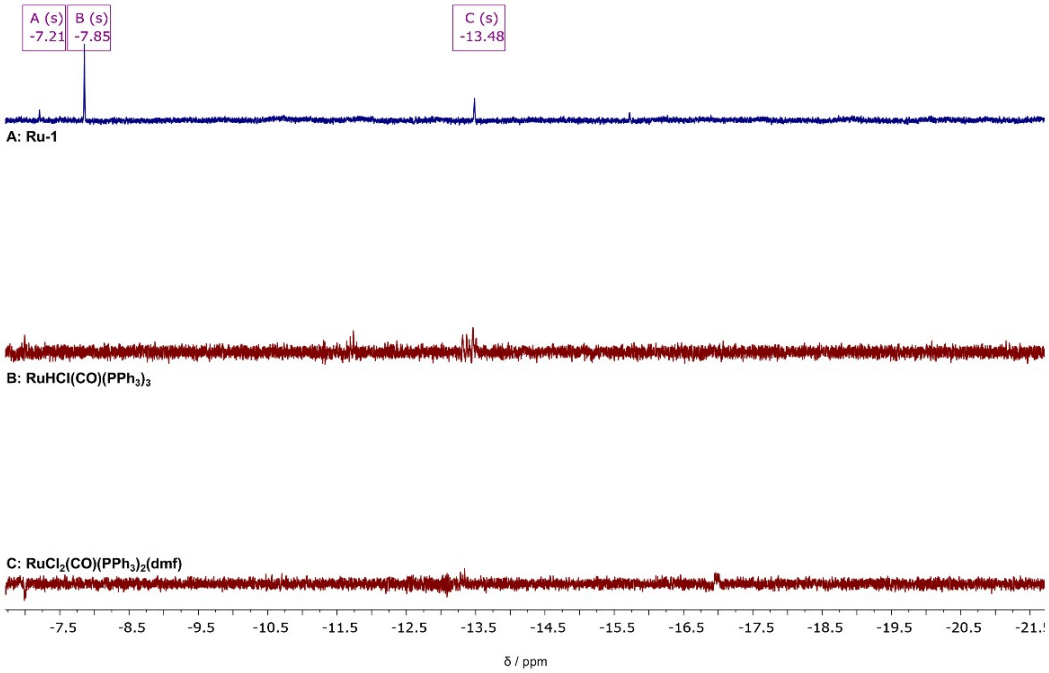

Figure S18b. Stacked *in situ* ^{1}H NMR spectra after 45 minutes of the second cycle of the FADH, showing the hydride region. Reaction conditions for **A**: EMIM $PO_2(OEt)_2$ (1 mL), **Ru-1** (0.1 mol%), FA (0.5 mL), 90 °C, cycle 1, 45 minutes; **B:** EMIM $PO_2(OEt)_2$ (1 mL), **RuHCl(CO)(PPh$_3$)$_3$** (0.1 mol%), FA (0.5 mL), 90 °C, cycle 1, 45 minutes; **C:** EMIM $PO_2(OEt)_2$ (1 mL), **RuCl$_2$(CO)(PPh$_3$)$_2$(dmf)** (0.1 mol%), FA (0.5 mL), 90 °C, cycle 1, 45 minutes.

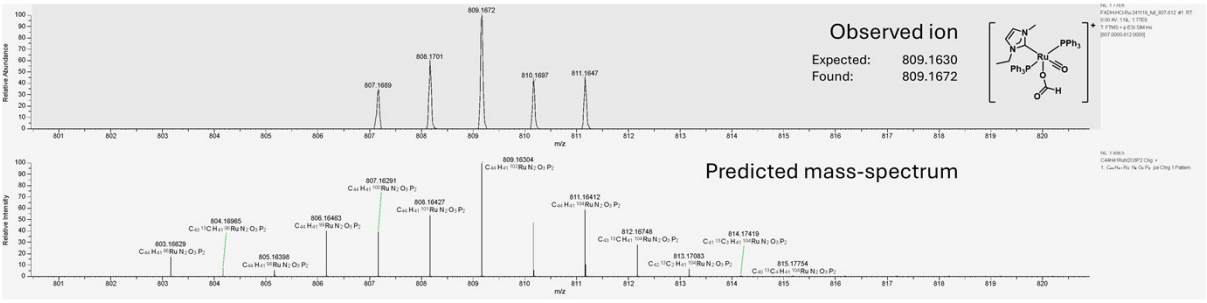

Figure S19a. *In situ* HR-MS spectrum of reaction mixture after 45 minutes during the first cycle using **$RuHCl(CO)(PPh_3)_3$** as (pre) catalyst, showing the region responsible for a suggested formato-fragment.

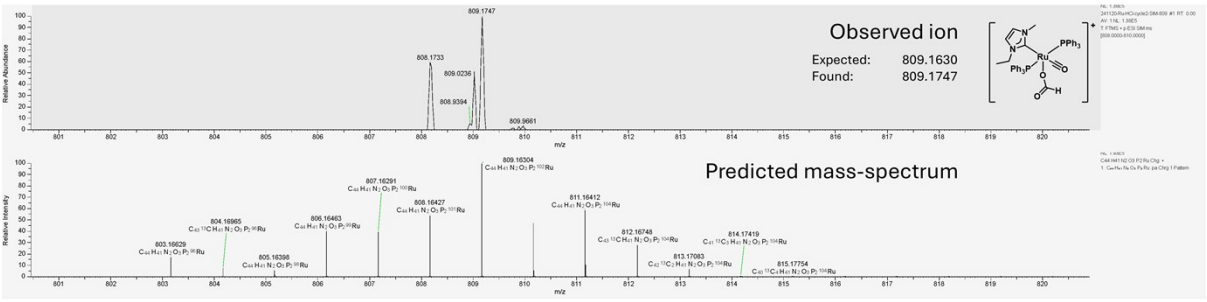

Figure S19b. *In situ* HR-MS spectrum of reaction mixture after 2 cycles and 3 hours using **$RuHCl(CO)(PPh_3)_3$** as (pre) catalyst, showing the region responsible for a suggested formato-fragment.

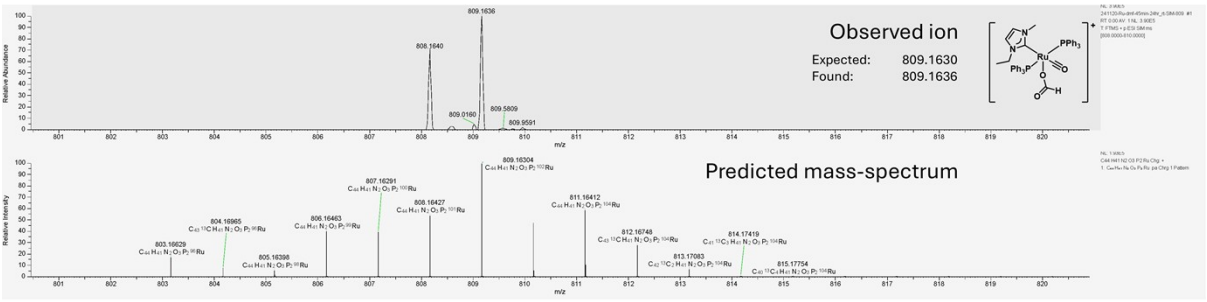

Figure S19c. *In situ* HR-MS spectrum of reaction mixture after 45 minutes during the first cycle using **$RuCl_2(CO)(PPh_3)_2$(dmf)** as (pre) catalyst, showing the region responsible for a suggested formato-fragment.

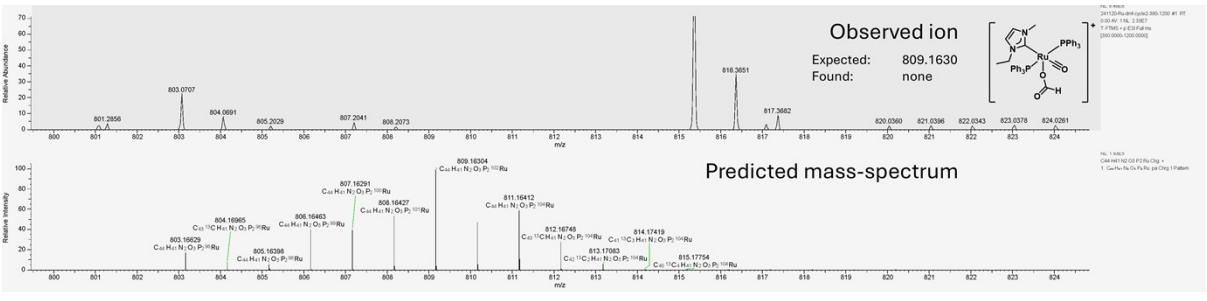

Figure S19d. *In situ* HR-MS spectrum of reaction mixture after 2 cycles and 3 hours using **$RuCl_2(CO)(PPh_3)_2$(dmf)** as (pre) catalyst, showing the region responsible for a suggested formato-fragment.

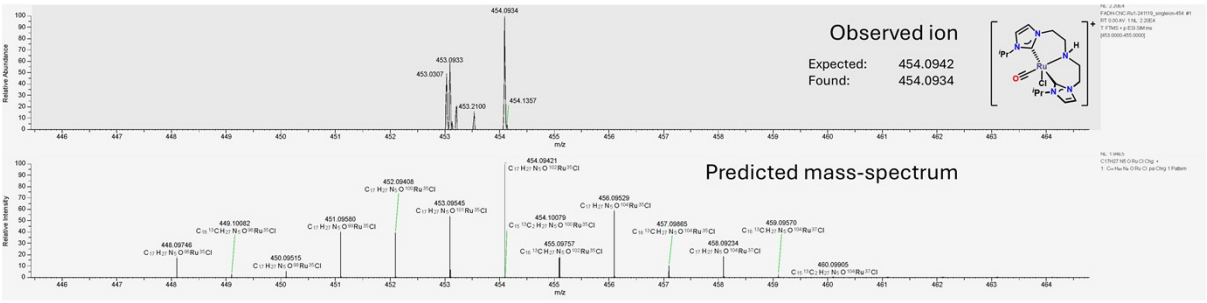

Figure S19e. *In situ* HR-MS spectrum of reaction mixture after 45 minutes during the first cycle using **Ru-1** as (pre) catalyst, showing the region responsible for a suggested chlorido-fragment.

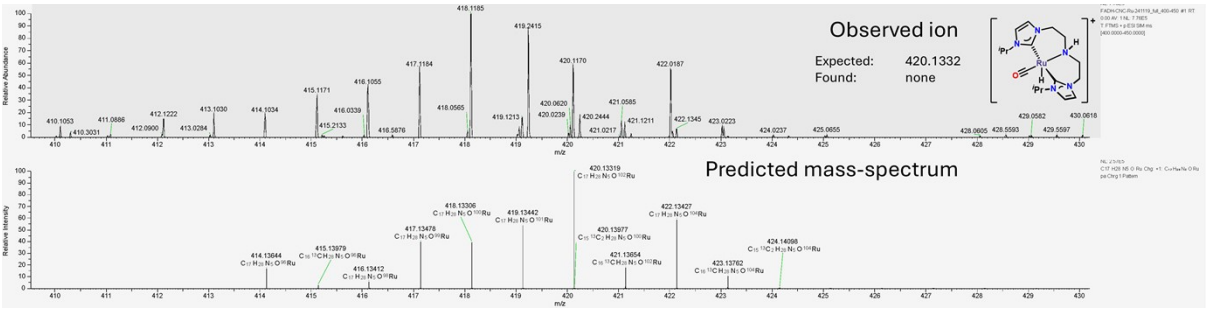

Figure S19f. *In situ* HR-MS spectrum of reaction mixture after 45 minutes during the first cycle using **Ru-1** as (pre) catalyst, showing the region responsible for a suggested hydrido-fragment.

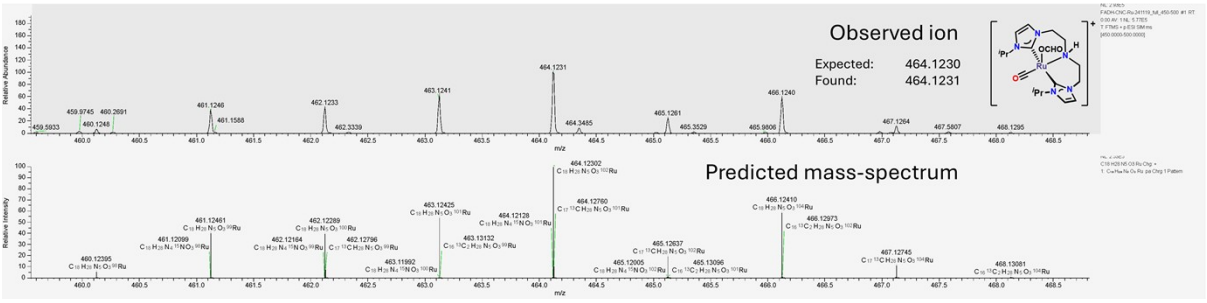

Figure S19g. *In situ* HR-MS spectrum of reaction mixture after 45 minutes during the first cycle using **Ru-1** as (pre) catalyst, showing the region responsible for a suggested formato-fragment.

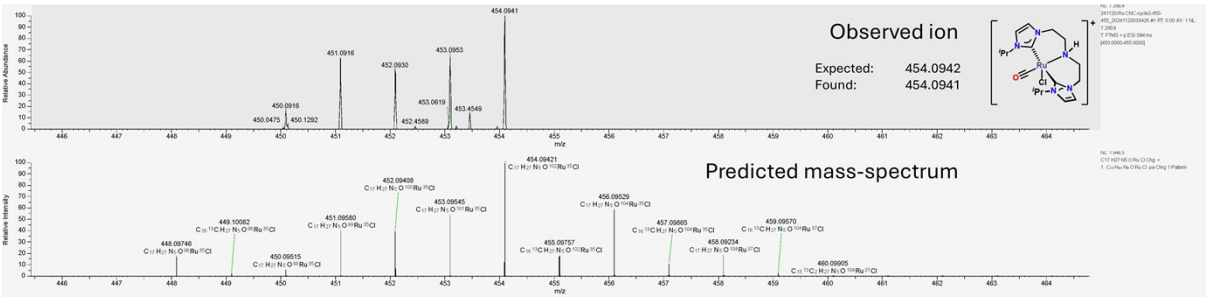

Figure S19h. *In situ* HR-MS spectrum of reaction mixture after 2 cycles and 3 hours using **Ru-1** as (pre) catalyst, showing the region responsible for a suggested chlorido-fragment.

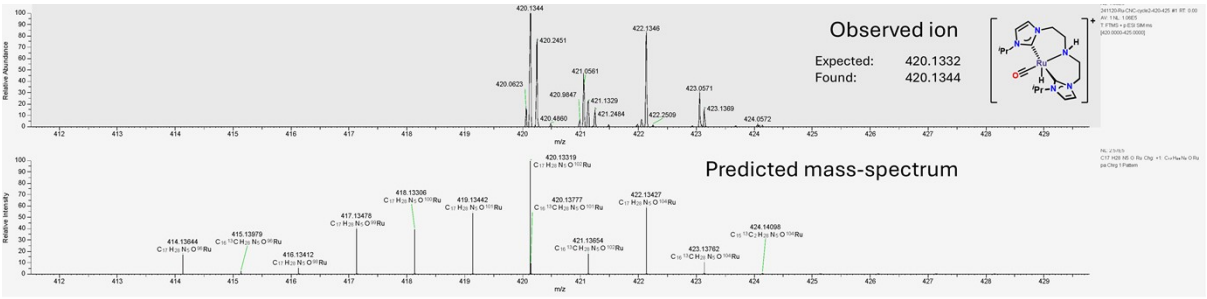

Figure S19i. *In situ* HR-MS spectrum of reaction mixture after 2 cycles and 3 hours using **Ru-1** as (pre) catalyst, showing the region responsible for a suggested hydrido-fragment.

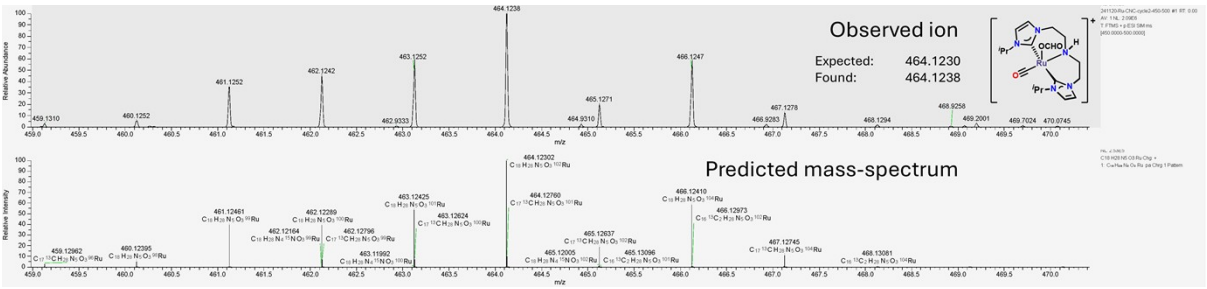

Figure S19j. *In situ* HR-MS spectrum of reaction mixture after 2 cycles and 3 hours using **Ru-1** as (pre) catalyst, showing the region responsible for a suggested formato-fragment.

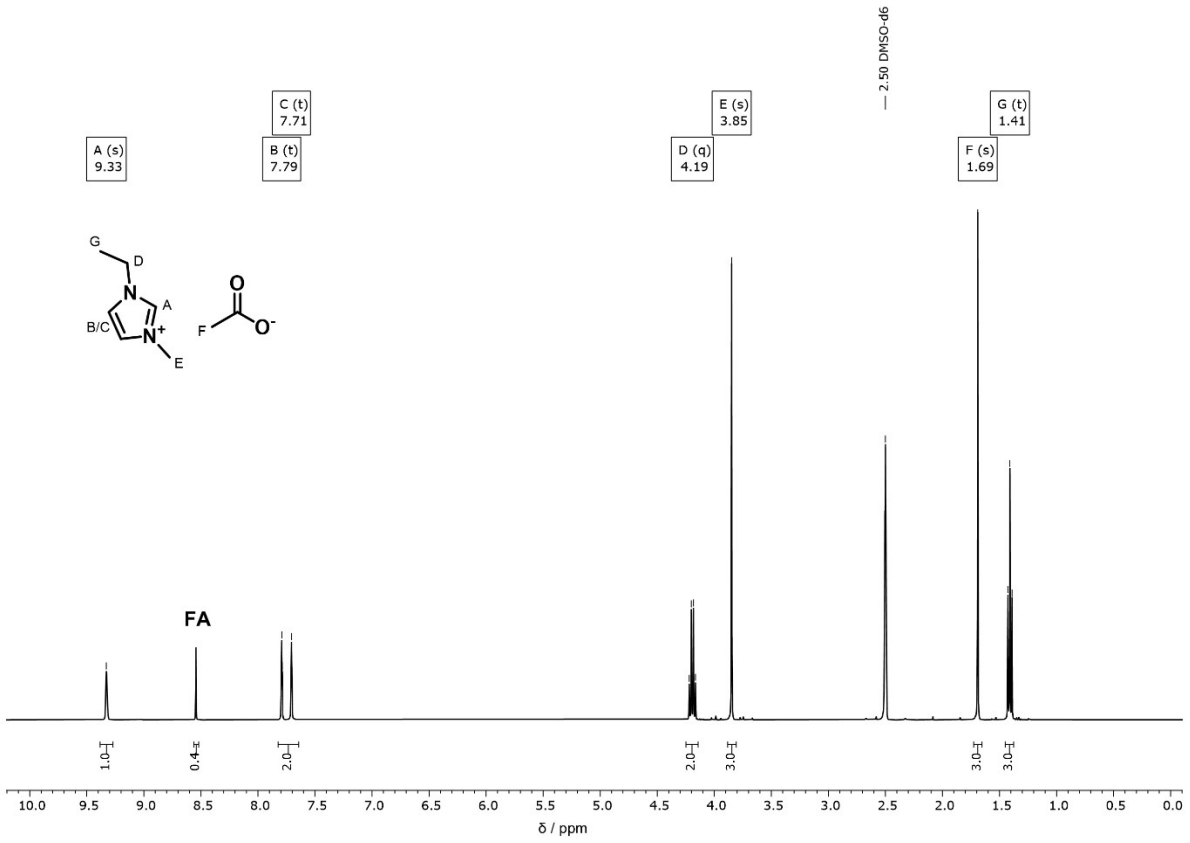

Figure S20. Example of ^{1}H NMR of FADH in EMIM OAc (1 mL IL, 0.5 mL FA, 0.05 mol% **Ru-1**, 100 °C, 1 h, 80% conversion).

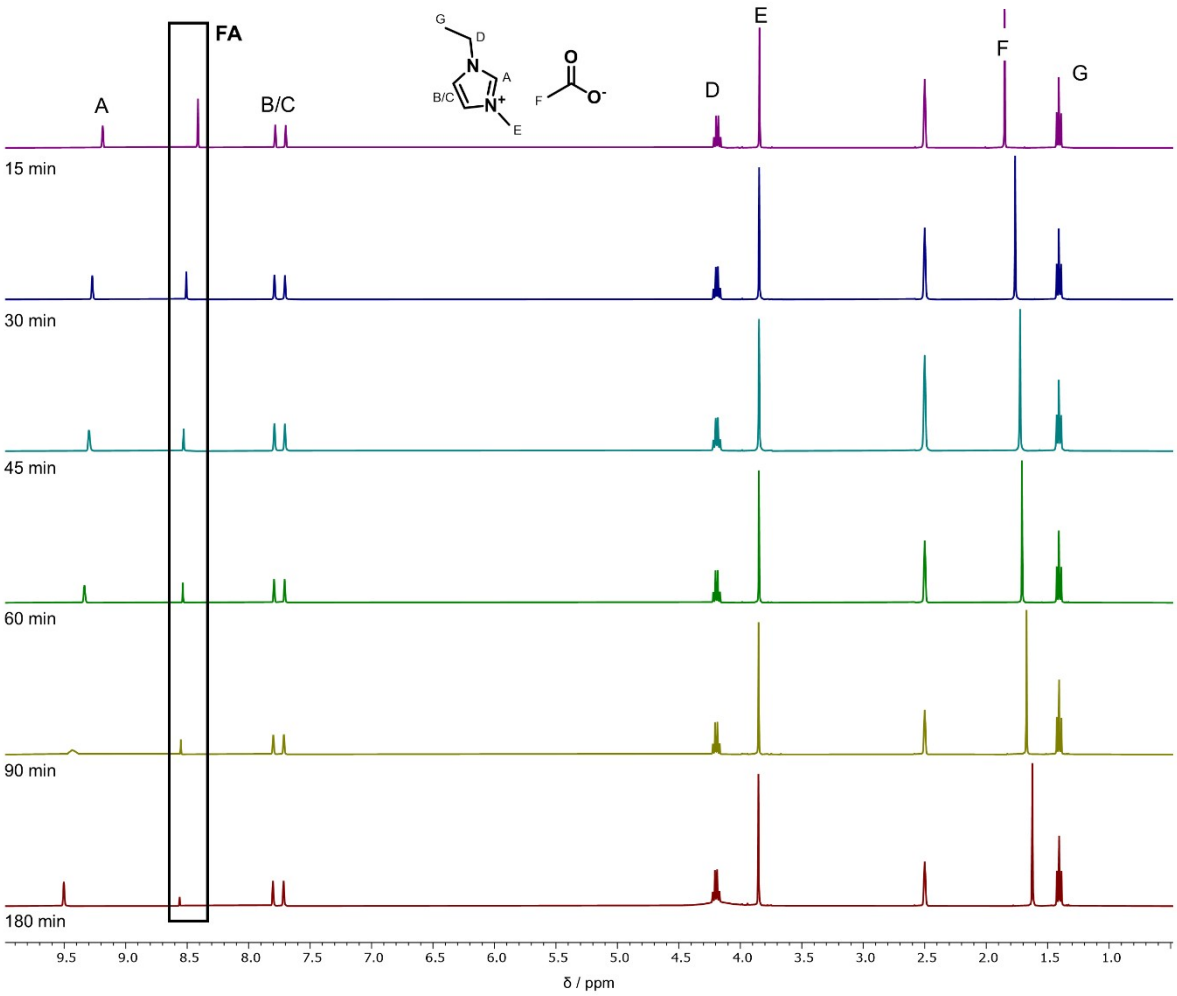

Figure S21. Example of stacked ^{1}H NMR spectra of FADH in EMIM OAc over 3 h (1 mL IL, 0.5 mL FA, 0.1 mol% **Ru-1**, 90 °C).

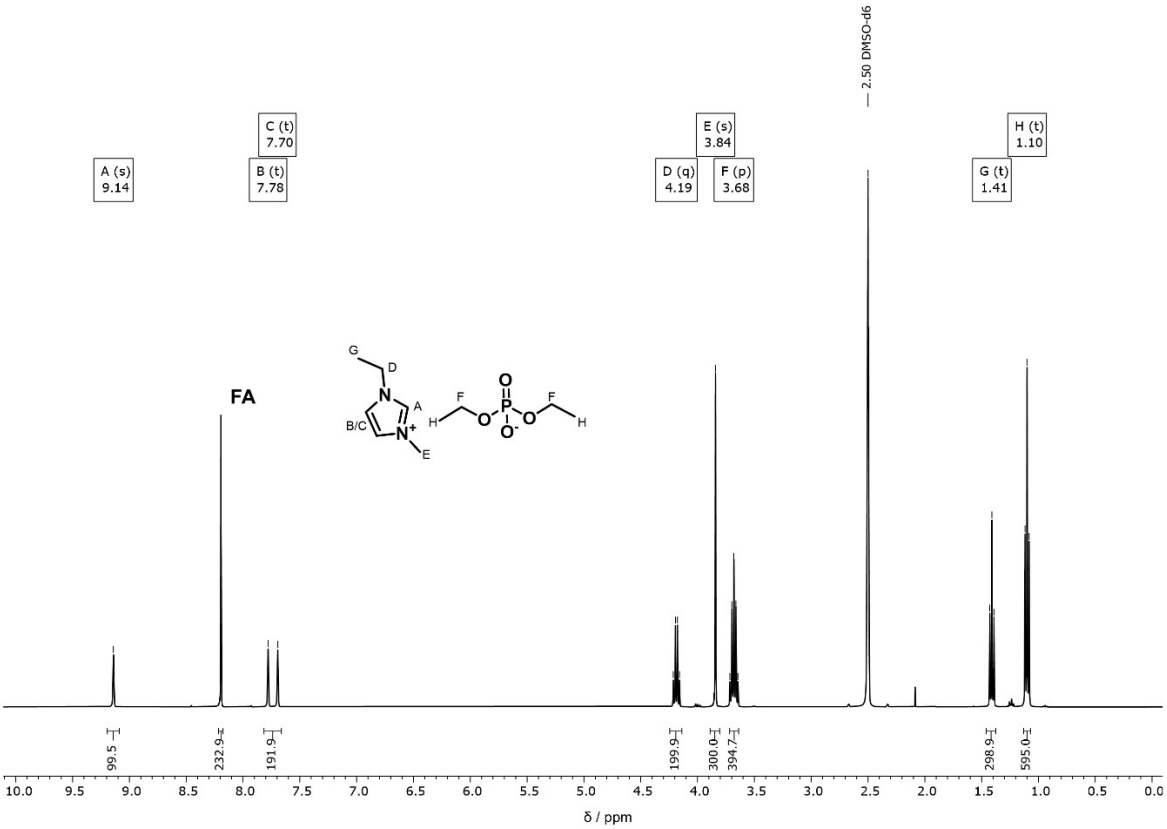

Figure S22a. Example of ^{1}H NMR of FADH in EMIM $PO_2(OEt)_2$ (1 mL IL, 0.5 mL FA, 0.1 mol% **Ru-1**, 100 °C, 15 min, 20% conversion) (Integral: 1H = 100).

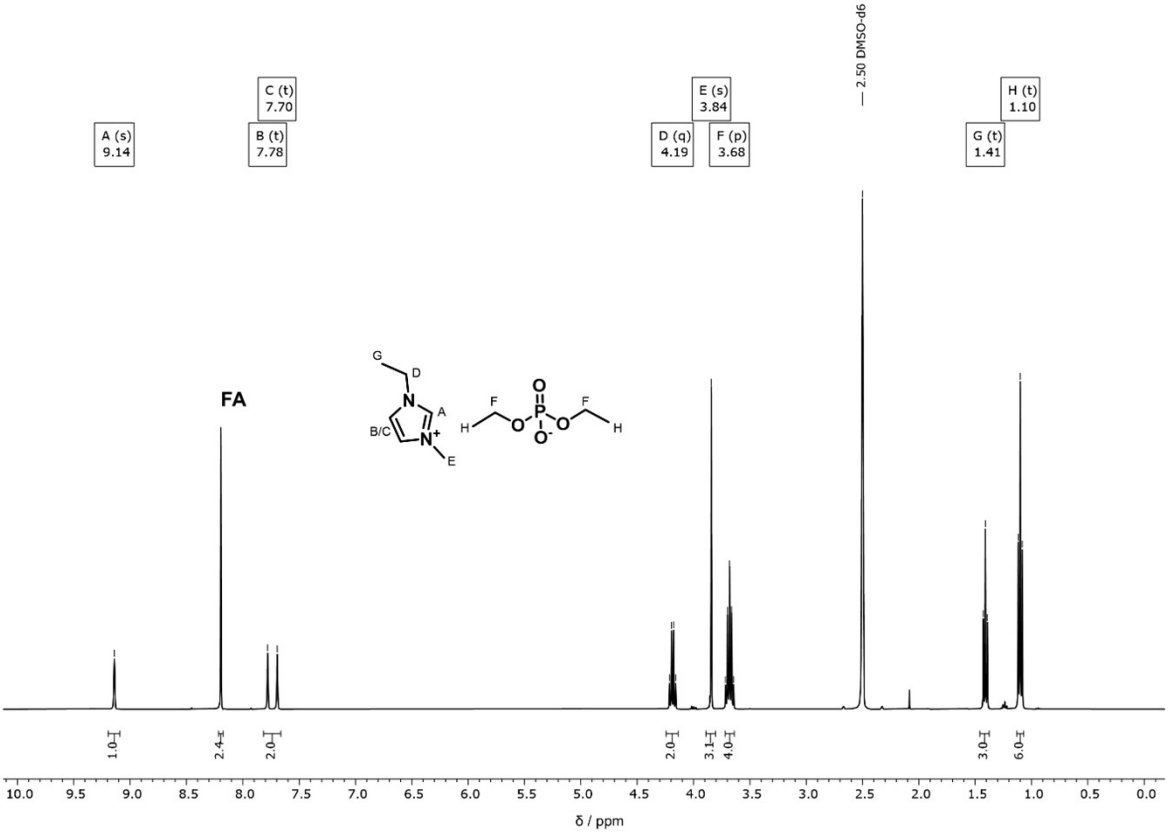

Figure S22b. Example of ^{1}H NMR of FADH in EMIM $PO_2(OEt)_2$ (1 mL IL, 0.5 mL FA, 0.1 mol% **Ru-1**, 100 °C, 15 min, 20% conversion) (Integral: 1 H = 1)

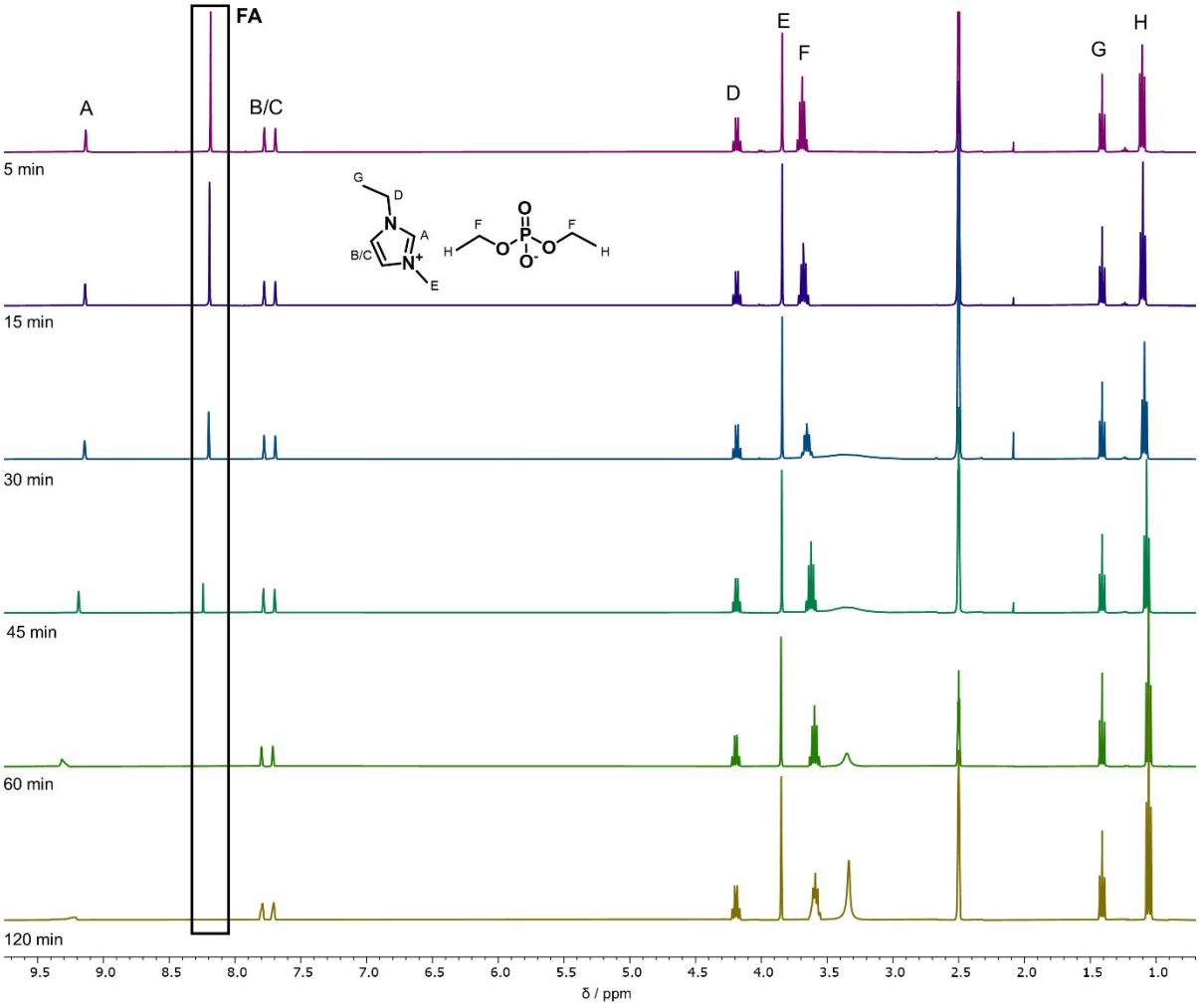

Figure S23. Example of stacked ^{1}H NMR spectra of FADH in EMIM $PO_2(OEt)_2$ over 2 h (1 mL IL, 0.5 mL FA, 0.1 mol% **Ru-1**, 100 °C).

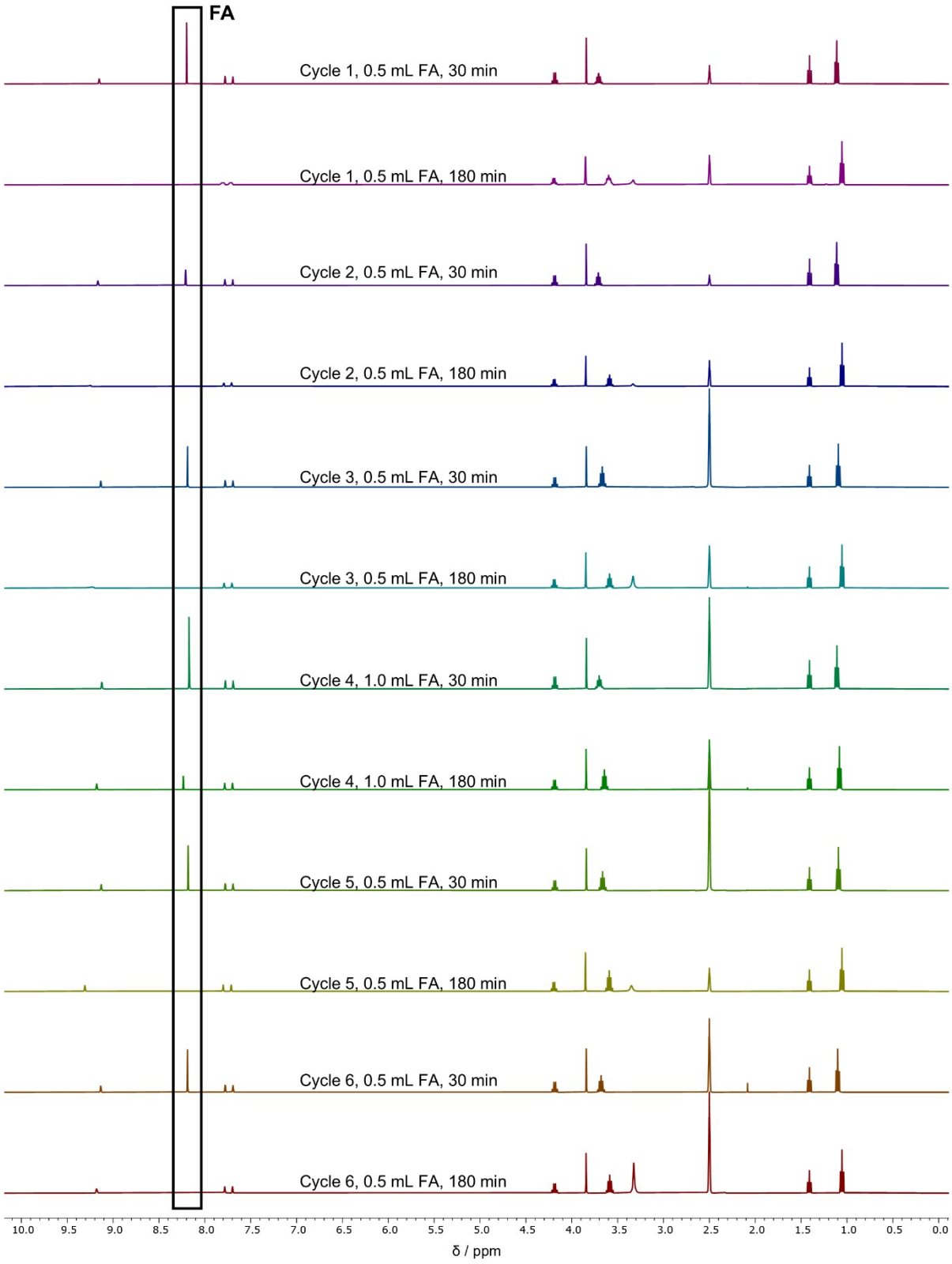

Figure S24. Stacked ^{1}H NMR spectra of FADH cycles in EMIM $PO_2(OEt)_2$ at 90°C and with 0.1 mol% **Ru-1** and 0.5- or 0.1-mL FA recorded after 30 and 180 min.

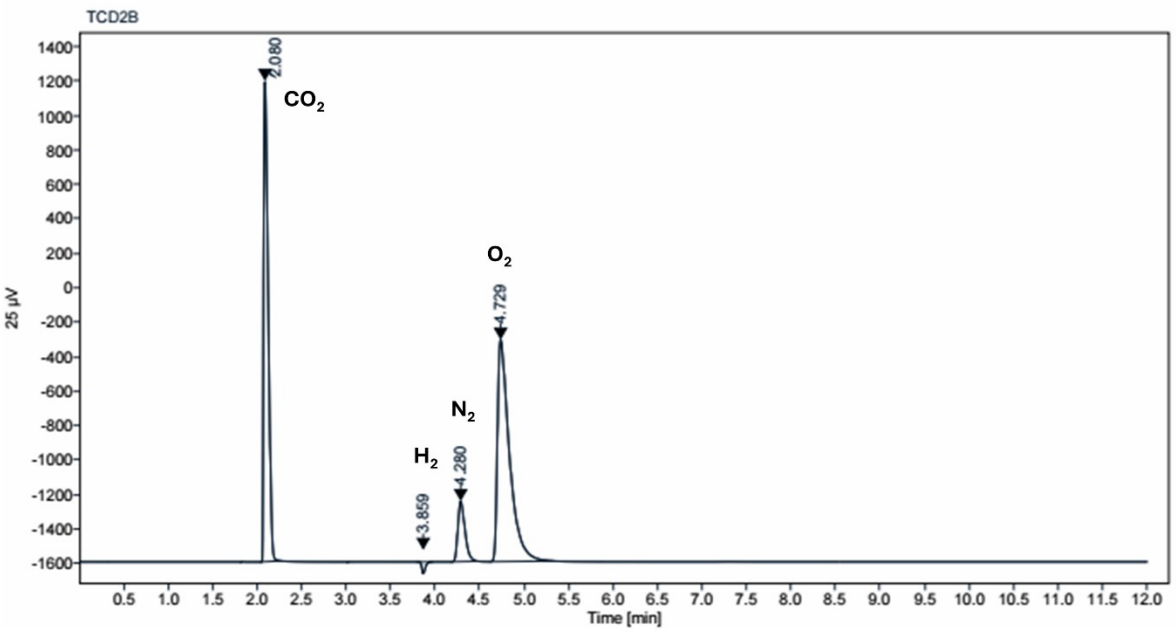

Figure S25a. GC-TCD report of FA dehydrogenation after 1 h at 90 °C in EMM $PO_2(OEt)_2$ with 0.1 mol% **$RuCl_2(PPh_3)_2(dmf)$** and using 0.5 mL FA.

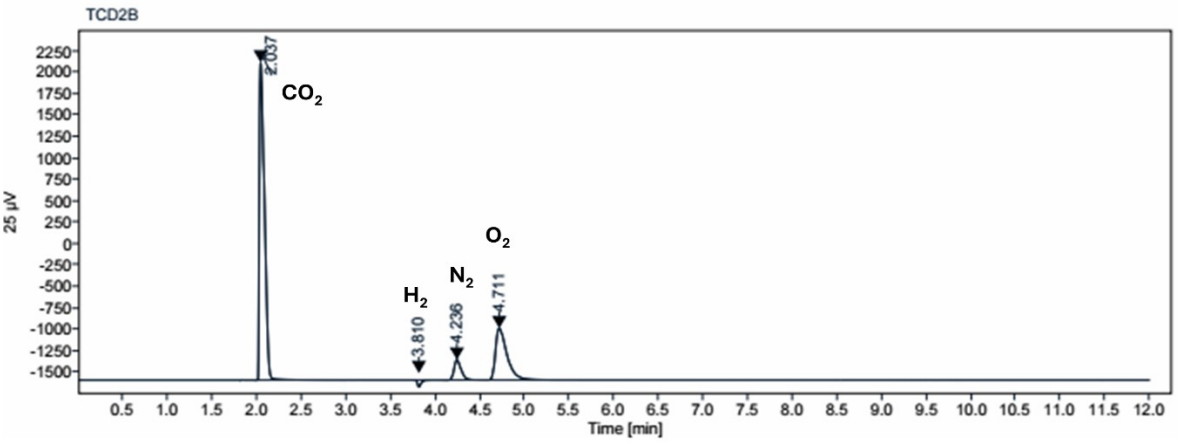

Figure S25b. GC-TCD report of FA dehydrogenation after 1 h at 90 °C in EMM $PO_2(OEt)_2$ with 0.1 mol% **$RuHCl(CO)(PPh_3)_3$** and using 0.5 mL FA

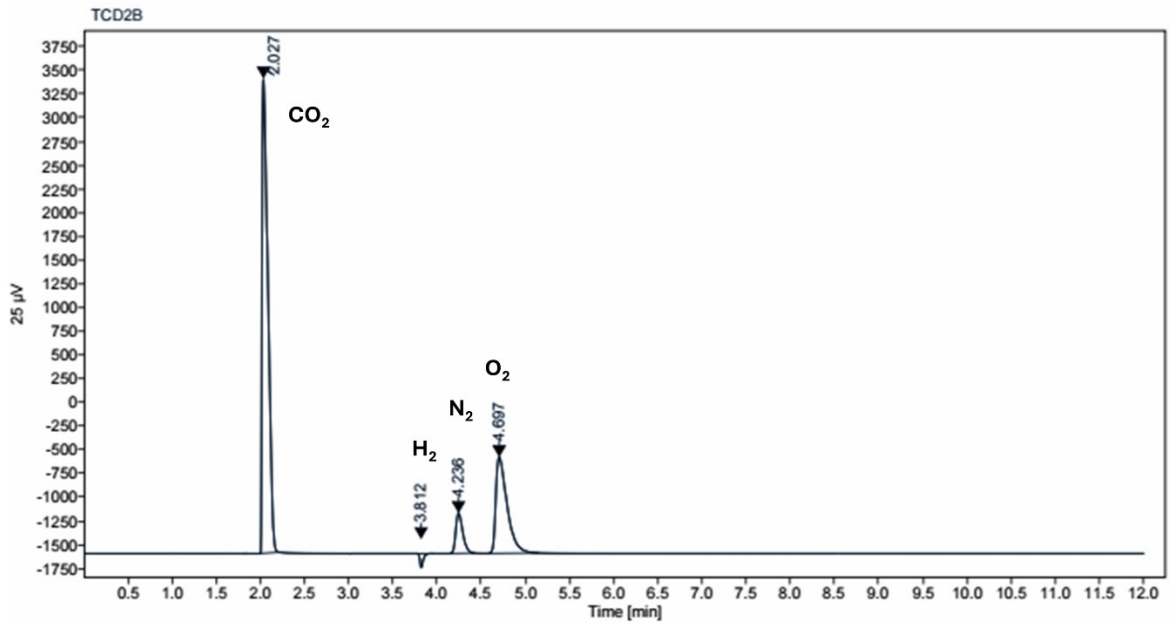

Figure S25c. GC-TCD report of FA dehydrogenation after 1 h at 90 °C in EMM $PO_2(OEt)_2$ with 0.1 mol% **Ru-1** and using 0.5 mL FA**.**

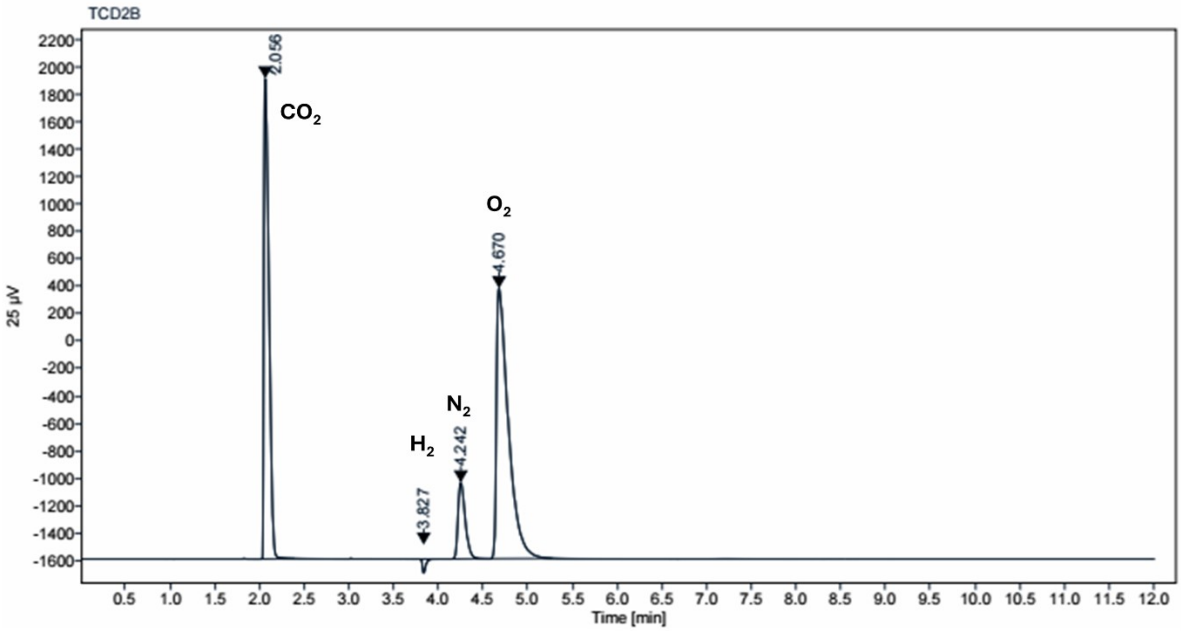

Figure S25d. GC-TCD report of FA dehydrogenation after 1 h at 100 °C in EMM $PO_2(OEt)_2$ with 0.1 mol% **Ru-1** and using 0.5 mL FA

Table S6. FA Dehydrogenation over time in EMIM OAc at 80 °C with **Ru-1** (0.1 mol%). [a]

Entry	Time	Conv. [%][b]	TON	TOF (h^{-1})
1	15 min	2	20	80
2	30 min	20	200	400
3	45 min	50	500	670
4	1 h	66	660	660
5	2 h	76	760	380
6	3 h	83	830	280

[a]Reaction conditions: **Ru-1** (0.1 mol%), EMIM OAc (1 mL), FA (13.3 mmol, 0.5 mL), 80 °C.
[b]Determined by ^{1}H-NMR.

Table S7. FA Dehydrogenation over time in EMIM OAc at 90 °C with **Ru-1** (0.1 mol%). [a]

Entry	Time	Conv. [%][b]	TON	TOF (h^{-1})
1	15 min	37	370	1480
2	30 min	68	680	1360
3	45 min	75	750	1000
4	1 h	78	780	780
5	2 h	84	840	420
6	3 h	91	910	300

[a]Reaction conditions: **Ru-1** (0.1 mol%), EMIM OAc (1 mL), FA (13.3 mmol, 0.5 mL), 90 °C.
[b]Determined by ^{1}H-NMR.

Table S8. FA Dehydrogenation over time in EMIM OAc at 100 °C with **Ru-1** (0.1 mol%). [a]

Entry	Time	Conv. [%][b]	TON	TOF (h^{-1})
1	15 min	66	660	2650
2	30 min	77	770	1550
3	45 min	81	810	1080
4	1 h	88	880	880
5	2 h	90	900	450
6	3 h	93	930	310

[a]Reaction conditions: **Ru-1** (0.1 mol%), EMIM OAc (1 mL), FA (13.3 mmol, 0.5 mL), 100 °C.
[b]Determined by ^{1}H-NMR.

Table S9. FA Dehydrogenation over time in EMIM OAc at 90 °C with **Ru-1** (0.05 mol%). [a]

Entry	Time	Conv. [%][b]	TON	TOF (h^{-1})
1	15 min	18	360	1440
2	30 min	40	800	1610
3	45 min	61	1220	1630
4	1 h	70	1400	1400
5	2 h	81	1630	810
6	3 h	86	1730	570

[a]Reaction conditions: **Ru-1** (0.05 mol%), EMIM OAc (1 mL), FA (13.3 mmol, 0.5 mL), 90 °C.
[b]Determined by ^{1}H-NMR.

Table S10. FA Dehydrogenation over time in EMIM OAc at 90 °C with **Ru-1** (0.025 mol%). [a]

Entry	Time	Conv. [%][b]	TON	TOF (h^{-1})
1	15 min	8	320	1290
2	30 min	20	810	1610
3	45 min	34	1370	1830
4	1 h	50	2010	2010
5	2 h	64	2580	1290
6	3 h	73	2940	980

[a]Reaction conditions: **Ru-1** (0.025 mol%), EMIM OAc (1 mL), FA (13.3 mmol, 0.5 mL), 90 °C.
[b]Determined by ^{1}H-NMR.

Table S11. FA Dehydrogenation over time in EMIM OAc at 100 °C with **Ru-1** (0.05 mol%). [a]

Entry	Time	Conv. [%][b]	TON	TOF (h^{-1})
1	15 min	44	880	3530
2	30 min	71	1420	2850
3	45 min	77	1550	2060
4	1 h	80	1610	1610
5	2 h	87	1750	880
6	3 h	90	1810	600

[a]Reaction conditions: **Ru-1** (0.05 mol%), EMIM OAc (1 mL), FA (13.3 mmol, 0.5 mL), 100 °C.
[b]Determined by ^{1}H-NMR.

Table S12. FA Dehydrogenation over time in EMIM $PO_2(OEt)_2$ at 90 °C with **Ru-1** (0.1 mol%).[a]

Entry	Time	Conv. [%][b]	TON	TOF (h^{-1})
1	15 min	10	100	400
2	30 min	10	100	200
3	45 min	14	140	190
4	1 h	21	210	210
5	2 h	60	600	300
6	3 h	>99	1000	330

[a]Reaction conditions: **Ru-1** (0.1 mol%), EMIM $PO_2(OEt)_2$ (1 mL), FA (13.3 mmol, 0.5 mL), 90 °C. [b]Determined by ^{1}H-NMR.

Table S13. FA Dehydrogenation over time in EMIM $PO_2(OEt)_2$ at 100 °C with **Ru-1** (0.1 mol%).[a]

Entry	Time	Conv. [%][b]	TON	TOF (h^{-1})
1	15 min	21	210	840
2	30 min	46	460	920
3	45 min	82	820	1100
4	1 h	99	990	990
5	2 h	99	990	500
6	3 h	>99	1000	330

[a]Reaction conditions: **Ru-1** (0.1 mol%), EMIM $PO_2(OEt)_2$ (1 mL), FA (13.3 mmol, 0.5 mL), 100 °C. [b]Determined by ^{1}H-NMR.

Table S14. FA Dehydrogenation over time in EMIM $PO_2(OEt)_2$ at 100 °C with **Ru-1** (0.05 mol%).[a]

Entry	Time	Conv. [%][b]	TON	TOF (h^{-1})
1	15 min	3	60	240
2	30 min	9	180	360
3	45 min	21	420	560
4	1 h	27	540	540
5	2 h	82	1650	830
6	3 h	99	2000	660

[a]Reaction conditions: **Ru-1** (0.05 mol%), EMIM $PO_2(OEt)_2$ (1 mL), FA (13.3 mmol, 0.5 mL), 100 °C. [b]Determined by ^{1}H-NMR.

Table S15. Second cycle for the FADH using the optimized catalytic system of **Ru-1** in EMIM $PO_2(OEt)_2$ at 90 °C.[a]

Entry	Time	Conv. [%][b]	TON	TOF (h^{-1})
1	15 min	12	120	470
2	30 min	25	250	500
3	45 min	42	420	560
4	1 h	65	650	650
5	2 h	>99	1000	500
6	3 h	>99	1000	330

[a]Standard reaction conditions: **Ru-1** (0.1 mol% in first cycle), EMIM $PO_2(OEt)_2$ (1 mL), FA (0.5 mL), 90 °C, 3 h under gentle flow of Ar. In each cycle, 0.5 mL FA is added. The solution is stirred overnight at 90 °C between finishing a cycle and commencing the next. [b]Determined by ^{1}H-NMR.

Table S16. Third cycle for the FADH using the optimized catalytic system of **Ru-1** in EMIM $PO_2(OEt)_2$ at 90 °C.[a]

Entry	Time	Conv. [%][b]	TON	TOF (h^{-1})
1	15 min	11	110	440
2	30 min	19	190	380
3	45 min	34	340	450
4	1 h	54	540	540
5	2 h	>99	990	500
6	3 h	>99	1000	330

[a]Standard reaction conditions: **Ru-1** (0.1 mol% in first cycle), EMIM $PO_2(OEt)_2$ (1 mL), FA (0.5 mL), 90 °C, 3 h under gentle flow of Ar. In each cycle, 0.5 mL FA is added. The solution is stirred overnight at 90 °C between finishing a cycle and commencing the next.
[b]Determined by ^{1}H-NMR.

Table S17. Fourth cycle for the FADH using the optimized catalytic system of **Ru-1** in EMIM $PO_2(OEt)_2$ at 90 °C.[a]

Entry	Time	Conv. [%][b]	TON	TOF (h^{-1})
1	15 min	25	500	2010
2	30 min	26	520	1040
3	45 min	nd[c]	nd	nd
4	1 h	20	400	400
5	2 h	50	1000	500
6	3 h	85	1710	570

[a]Standard reaction conditions: **Ru-1** (0.1 mol% in first cycle), EMIM $PO_2(OEt)_2$ (1 mL), FA (1.0 mL), 90 °C, 3 h under gentle flow of Ar. In the fourth cycle, 1.0 mL FA is added. The solution is stirred overnight at 90 °C between finishing a cycle and commencing the next.
[b]Determined by ^{1}H-NMR.
[c]Not determined

Table S18. Fifth cycle for the FADH using the optimized catalytic system of **Ru-1** in EMIM $PO_2(OEt)_2$ at 90 °C.[a]

Entry	Time	Conv. [%][b]	TON	TOF (h^{-1})
1	15 min	2	20	80
2	30 min	9	90	180
3	45 min	17	170	380
4	1 h	25	250	250
5	2 h	99	1000	500
6	3 h	>99	1000	330

[a]Standard reaction conditions: **Ru-1** (0.1 mol% in first cycle), EMIM $PO_2(OEt)_2$ (1 mL), FA (0.5 mL), 90 °C, 3 h under gentle flow of Ar. In each cycle, 0.5 mL FA is added. The solution is stirred overnight at 90 °C between finishing a cycle and commencing the next.
[b]Determined by ^{1}H-NMR.

Table S19. Sixth cycle for the FADH using the optimized catalytic system of **Ru-1** in EMIM $PO_2(OEt)_2$ at 90 °C.[a]

Entry	Time	Conv. [%][b]	TON	TOF (h^{-1})
1	15 min	nd	nd	nd
2	30 min	8	80	160
3	45 min	11	110	150
4	1 h	23	230	230
5	2 h	98	980	490
6	3 h	100	1000	330

[a]Standard reaction conditions: **Ru-1** (0.1 mol% in first cycle), EMIM $PO_2(OEt)_2$ (1 mL), FA (0.5 mL), 90 °C, 3 h under gentle flow of Ar. In each cycle, 0.5 mL FA is added. The solution is stirred overnight at 90 °C between finishing a cycle and commencing the next.
[b]Determined by ^{1}H-NMR.

Table 19b. FADH cycles using the optimised catalytic system of **Ru-1** in EMIM $PO_2(OEt)_2$.[a]

Cycle	FA [mL]	Conv. [%][b]	TON	Accumulated TON	TOF_{max} [h^{-1}]
1	0.5	>99	1000	-	400
2	0.5	>99	1000	2000	650
3	0.5	>99	1000	3000	540
4[c]	1.0	85	1706[d]	4710	2010
5	0.5	>99	1000	5710	500
6	0.5	>99	1000	6710	490

[a]Standard reaction conditions: **Ru-1** (0.1 mol% in first cycle), EMIM $PO_2(OEt)_2$ (1 mL), FA (0.5 or 1.0 mL), 90 °C, 3 h under gentle flow of Ar. Gas composition is analysed by GC-TCD. In each cycle, 0.5 mL FA is added. The solution is stirred overnight at 90 °C between finishing a cycle and commencing the next. [b]Determined by ^{1}H-NMR. [c]1 mL FA added after leaving the solution of the catalyst in IL stirring overnight at 90 °C. [d]The remaining FA is fully dehydrogenated in the subsequent period before the next cycle.

Table S20. FA Dehdrogenation over time in EMIM $PO_2(OEt)_2$ at 90 °C with **$RuCl_2(CO)(PPh_3)_2(dmf)$** (0.1 mol%).[a]

Entry	Time	Conv. [%][b]	TON	TOF (h^{-1})
1	15 min	24	240	960
2	30 min	30	300	600
3	45 min	44	440	590
4	1 h	>99	1000	1000
5	2 h	>99	1000	500
6	3 h	>99	1000	330

[a]Reaction conditions: **$RuCl_2(CO)(PPh_3)_2(dmf)$** (0.1 mol%), EMIM $PO_2(OEt)_2$ (1 mL), FA (13.3 mmol, 0.5 mL), 90 °C. [b]Determined by ^{1}H-NMR.

Table S21. FA Dehydrogenation over time in EMIM $PO_2(OEt)_2$ at 90 °C with **$RuCl_2(CO)(PPh_3)_2$(dmf)** (0.1 mol%).[a]

Entry	Time	Conv. [%][b]	TON	TOF (h^{-1})
1	15 min	18	180	720
2	30 min	23	230	460
3	45 min	31	310	410
4	1 h	33	330	330
5	2 h	99	1000	500
6	3 h	99	1000	330

[a]Reaction conditions: **$RuCl_2(CO)(PPh_3)_2$(dmf)** (0.1 mol%), EMIM PO_2 $(OEt)_2$ (1 mL), adding 0.5 mL more of FA (13.3 mmol) after leaving the catalytic system stirring overnight at 90 °C [b]Determined by ^{1}H-NMR.

Table S22. FA Dehydrogenation over time in EMIM $PO_2(OEt)_2$ at 90 °C with **$RuCl_2(CO)(PPh_3)_2$(dmf)** (0.1 mol%).[a]

Entry	Time	Conv. [%][b]	TON	TOF (h^{-1})
1	15 min	32	640	2570
2	30 min	34	680	1370
3	45 min	40	800	1070
4	1 h	45	900	900
5	2 h	49	980	490
6	3 h	53	1060	350

[a]Reaction conditions: **$RuCl_2(CO)(PPh_3)_2$(dmf)** (0.1 mol%), EMIM $PO_2(OEt)_2$ (1 mL), adding 1 mL more of FA (26.6 mmol) after leaving the catalytic system stirring overnight at 90 °C. [b]Determined by ^{1}H-NMR.

Table S23. Cycle 1. FA Dehydrogenation over time in EMIM $PO_2(OEt)_2$ at 90 °C with **$RuHCl(CO)(PPh_3)_3$** (0.1 mol%).

Entry	Time	Conv. [%][b]	TON	TOF (h^{-1})
1	15 min	17	170	680
2	30 min	17	170	340
3	45 min	27	270	360
4	1 h	35	350	350
5	2 h	>99	1000	500
6	3 h	>99	1000	330

[a]Reaction conditions: **$RuHCl(CO)(PPh_3)_3$** (0.1 mol%), EMIM $PO_2(OEt)_2$ (1 mL), FA (13.3 mmol, 0.5 mL), 90 °C. NMR error margin of 10%. [b]Determined by ^{1}H-NMR.

Table S24. Cycle 2. FA Dehydrogenation over time in EMIM $PO_2(OEt)_2$ at 90 °C with **$RuHCl(CO)(PPh_3)_3$** (0.1 mol%).

Entry	Time	Conv. [%][b]	TON	TOF (h^{-1})
1	15 min	15	150	600
2	30 min	19	190	380
3	45 min	20	200	270
4	1 h	20	200	200
5	2 h	26	260	130
6	3 h	36	360	120

[a]Reaction conditions: In each cycle, 0.5 mL FA is added. The solution is stirred overnight at 90 °C between finishing a cycle and commencing the next. **$RuHCl(CO)(PPh_3)_3$** (0.1 mol%), EMIM $PO_2(OEt)_2$ (1 mL), FA (13.3 mmol, 0.5 mL), 90 °C. NMR error margin of 10%. [b]Determined by ^{1}H-NMR.

Table S25. Cycle 3. FA Dehydrogenation over time in EMIM $PO_2(OEt)_2$ at 90 °C with **$RuHCl(CO)(PPh_3)_3$** (0.1 mol%).

Entry	Time	Conv. [%][b]	TON	TOF (h^{-1})
1	15 min	5	50	200
2	30 min	12	120	240
3	45 min	13	130	170
4	1 h	18	180	180
5	2 h	31	310	160
6	3 h	44	440	150

[a]Reaction conditions: In each cycle, 0.5 mL FA is added. The solution is stirred overnight at 90 °C between finishing a cycle and commencing the next. **$RuHCl(CO)(PPh_3)_3$** (0.1 mol%), EMIM $PO_2(OEt)_2$ (1 mL), FA (13.3 mmol, 0.5 mL), 90 °C. NMR error margin of 10%. [b]Determined by ^{1}H-NMR.

Table S26. Cycle 4. FA Dehydrogenation over time in EMIM $PO_2(OEt)_2$ at 90 °C with **$RuHCl(CO)(PPh_3)_3$** (0.1 mol%).

Entry	Time	Conv. [%][b]	TON	TOF (h^{-1})
1	15 min	9	180	720
2	30 min	19	380	760
3	45 min	24	480	640
4	1 h	24	480	480
5	2 h	39	780	390
6	3 h	52	1000	330

[a]Reaction conditions: 1 mL FA is added. The solution is stirred overnight at 90 °C between finishing a cycle and commencing the next. **$RuHCl(CO)(PPh_3)_3$** (0.1 mol%), EMIM $PO_2(OEt)_2$ (1 mL), FA (13.3 mmol, 0.5 mL), 90 °C. NMR error margin of 10%. [b]Determined by ^{1}H-NMR.

Table S27. Cycle 5. FA Dehydrogenation over time in EMIM $PO_2(OEt)_2$ at 90 °C with **$RuHCl(CO)(PPh_3)_3$** (0.1 mol%).

Entry	Time	Conv. [%][b]	TON	TOF (h^{-1})
1	15 min	0	-	-
2	30 min	0	-	-
3	45 min	2	20	30
4	1 h	6	60	60
5	2 h	15	150	80
6	3 h	25	250	80

[a]Reaction conditions: In each cycle, 0.5 mL FA is added. The solution is stirred overnight at 90 °C between finishing a cycle and commencing the next. **$RuHCl(CO)(PPh_3)_3$** (0.1 mol%), EMIM $PO_2(OEt)_2$ (1 mL), FA (13.3 mmol, 0.5 mL), 90 °C. NMR error margin of 10%. [b]Determined by ^{1}H-NMR.

Table S28. Cycle 6. FA Dehydrogenation over time in EMIM $PO_2(OEt)_2$ at 90 °C with **$RuHCl(CO)(PPh_3)_3$** (0.1 mol%).

Entry	Time	Conv. [%][b]	TON	TOF (h^{-1})
1	15 min	0	-	-
2	30 min	0	-	-
3	45 min	6	60	80
4	1 h	14	140	140
5	2 h	14	140	70
6	3 h	21	210	70

[a]Reaction conditions: In each cycle, 0.5 mL FA is added. The solution is stirred overnight at 90 °C between finishing a cycle and commencing the next. **$RuHCl(CO)(PPh_3)_3$** (0.1 mol%), EMIM $PO_2(OEt)_2$ (1 mL), FA (13.3 mmol, 0.5 mL), 90 °C. NMR error margin of 10%. [b]Determined by ^{1}H-NMR.

Table S29. Cycle 1. FA Dehydrogenation over time in EMIM $PO_2(OEt)_2$ at 90 °C with **$RuCl_2(CO)(PPh_3)_2$(dmf)** (0.1 mol%).

Entry	Time	Conv. [%][b]	TON	TOF (h^{-1})
1	15 min	27	270	1080
2	30 min	42	420	840
3	45 min	97	970	1300
4	1 h	>99	1000	1000
5	2 h	>99	1000	500
6	3 h	>99	1000	330

[a]Reaction conditions: Precursor **$RuCl_2(CO)(PPh_3)_2$(dmf)** (0.1 mol%), EMIM $PO_2(OEt)_2$ (1 mL), FA (13.3 mmol, 0.5 mL), 90 °C. NMR error margin of 10%. [b]Determined by ^{1}H-NMR.

Table S30. Cycle 2. FA Dehydrogenation over time in EMIM $PO_2(OEt)_2$ at 90 °C with **$RuCl_2(CO)(PPh_3)_2$(dmf)** (0.1 mol%).

Entry	Time	Conv. [%][b]	TON	TOF (h^{-1})
1	15 min	20	200	800
2	30 min	23	230	460
3	45 min	30	300	400
4	1 h	43	430	430
5	2 h	>99	1000	500
6	3 h	>99	1000	330

[a]Reaction conditions: In each cycle, 0.5 mL FA is added. The solution is stirred overnight at 90 °C between finishing a cycle and commencing the next. Precursor **$RuCl_2(CO)(PPh_3)_2$(dmf)** (0.1 mol%), EMIM $PO_2(OEt)_2$ (1 mL), FA (13.3 mmol, 0.5 mL), 90 °C. NMR error margin of 10%. [b]Determined by ^{1}H-NMR.

Table S31. Cycle 3. FA Dehydrogenation over time in EMIM $PO_2(OEt)_2$ at 90 °C with **$RuCl_2(CO)(PPh_3)_2$(dmf)** (0.1 mol%).

Entry	Time	Conv. [%][b]	TON	TOF (h^{-1})
1	15 min	22	220	880
2	30 min	22	220	440
3	45 min	25	250	330
4	1 h	27	270	270
5	2 h	70	700	350
6	3 h	>99	1000	330

[a]Reaction conditions: In each cycle, 0.5 mL FA is added. The solution is stirred overnight at 90 °C between finishing a cycle and commencing the next. Precursor **$RuCl_2(CO)(PPh_3)_2$(dmf)** (0.1 mol%), EMIM $PO_2(OEt)_2$ (1 mL), FA (13.3 mmol, 0.5 mL), 90 °C. NMR error margin of 10%. [b]Determined by ^{1}H-NMR.

Table S32. Cycle 4. FA Dehydrogenation over time in EMIM $PO_2(OEt)_2$ at 90 °C with **$RuCl_2(CO)(PPh_3)_2$(dmf)** (0.1 mol%).

Entry	Time	Conv. [%][b]	TON	TOF (h^{-1})
1	15 min	2	40	160
2	30 min	8	160	320
3	45 min	16	320	430
4	1 h	16	320	320
5	2 h	29	580	290
6	3 h	33	660	220

[a]Reaction conditions: 1 mL FA is added. The solution is stirred overnight at 90 °C between finishing a cycle and commencing the next. Precursor **$RuCl_2(CO)(PPh_3)_2$(dmf)** (0.1 mol%), EMIM $PO_2(OEt)_2$ (1 mL), FA (13.3 mmol, 0.5 mL), 90 °C. NMR error margin of 10%. [b]Determined by ^{1}H-NMR.

Table S33. Cycle 5. FA Dehydrogenation over time in EMIM PO_2 $(OEt)_2$ at 90 °C with **$RuCl_2(CO)(PPh_3)_2$(dmf)** (0.1 mol%).

Entry	Time	Conv. [%][b]	TON	TOF (h^{-1})
1	15 min	0	-	-
2	30 min	1	10	20
3	45 min	10	100	130
4	1 h	19	190	190
5	2 h	29	290	150
6	3 h	65	650	220

[a]Reaction conditions: In each cycle, 0.5 mL FA is added. The solution is stirred overnight at 90 °C between finishing a cycle and commencing the next. Precursor **$RuCl_2(CO)(PPh_3)_2$(dmf)** (0.1 mol%), EMIM PO_2 $(OEt)_2$ (1 mL), FA (13.3 mmol, 0.5 mL), 90 °C. NMR error margin of 10%. [b]Determined by ^{1}H-NMR.

Table S34. Cycle 6. FA Dehydrogenation over time in EMIM $PO_2(OEt)_2$ at 90 °C with **$RuCl_2(CO)(PPh_3)_2$(dmf)** (0.1 mol%).

Entry	Time	Conv. [%][b]	TON	TOF (h^{-1})
1	15 min	2	20	80
2	30 min	6	60	120
3	45 min	6	60	80
4	1 h	6	60	60
5	2 h	18	180	90
6	3 h	29	290	100

[a]Reaction conditions: In each cycle, 0.5 mL FA is added. The solution is stirred overnight at 90 °C between finishing a cycle and commencing the next. Precursor **$RuCl_2(CO)(PPh_3)_2$(dmf)** (0.1 mol%), EMIM $PO_2(OEt)_2$ (1 mL), FA (13.3 mmol, 0.5 mL), 90 °C. NMR error margin of 10%. [b]Determined by ^{1}H-NMR.

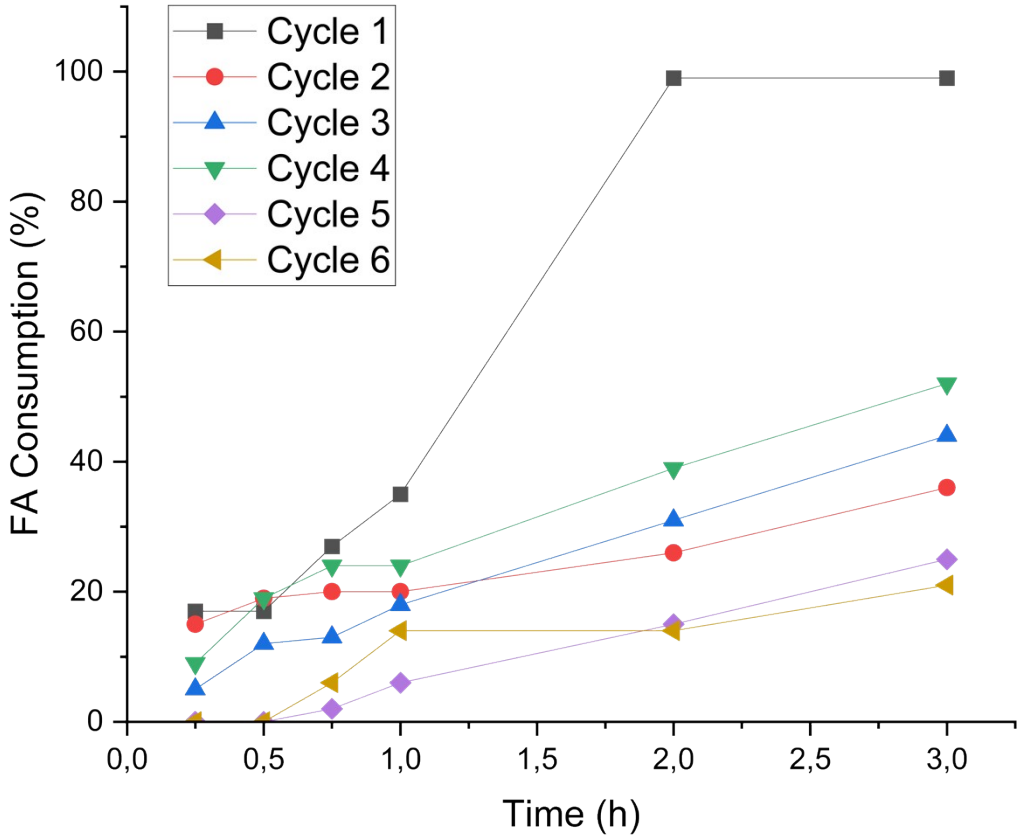

Figure S26. FADH cycles using the optimised catalytic system of **$RuHCl(CO)(PPh_3)_3$** in EMIM $PO_2(OEt)_2$.[a]

[a]Standard reaction conditions: **$Ru(H)(PPh_3)_3(CO)Cl$** (0.1 mol% in first cycle), EMIM $PO_2(OEt)_2$ (1 mL), FA (0.5 or 1.0 mL), 90 °C, 3 h under gentle flow of Ar. In each cycle, 0.5 mL FA is added. The solution is stirred overnight at 90 °C between finishing a cycle and commencing the next. In the fourth cycle 1 mL FA added after leaving the solution of the catalyst in IL stirring overnight at 90 °C.

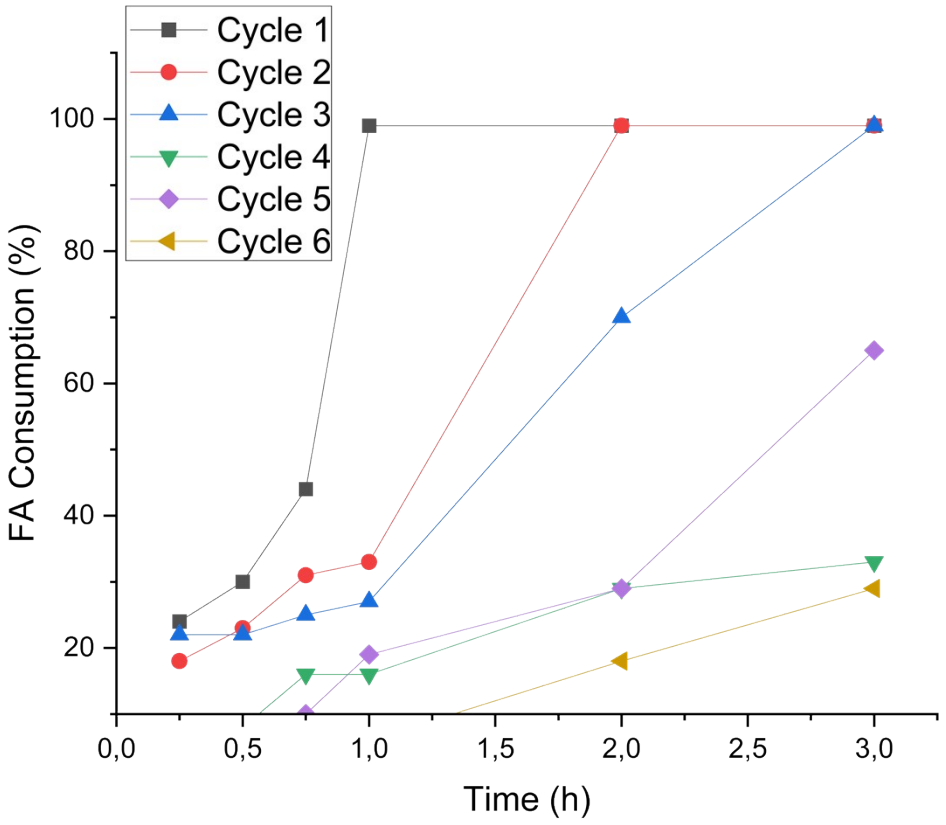

Figure S27. FADH cycles using the optimised catalytic system of **$RuCl_2(CO)(PPh_3)_2$(dmf)** in EMIM $PO_2(OEt)_2$.[a]

[a]Standard reaction conditions: **$RuCl_2(CO)(PPh_3)_2$(dmf)** (0.1 mol% in first cycle), EMIM $PO_2(OEt)_2$ (1 mL), FA (0.5 or 1.0 mL), 90 °C, 3 h under gentle flow of Ar. In each cycle, 0.5 mL FA is added. The solution is stirred overnight at 90 °C between finishing a cycle and commencing the next. In the fourth cycle 1 mL FA added after leaving the solution of the catalyst in IL stirring overnight at 90 °C.

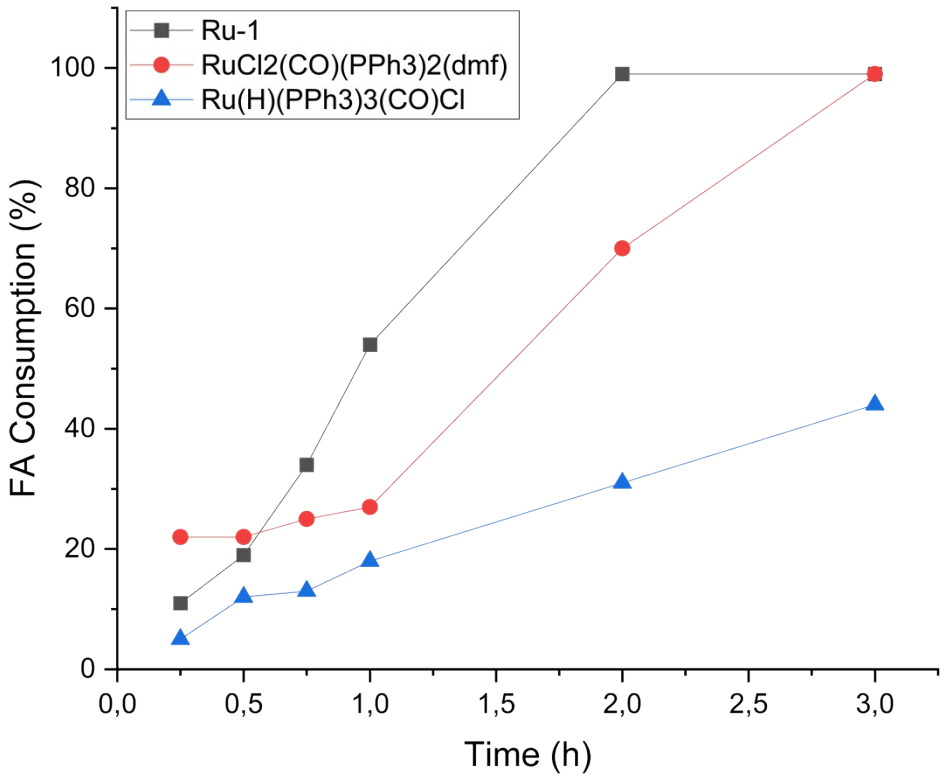

Figure S28. FADH third cycle. Comparison among the complexes tested.

[a]Standard reaction conditions: **Ru catalyst** (0.1 mol% in first cycle), EMIM $PO_2(OEt)_2$ (1 mL), FA (0.5 or 1.0 mL), 90 °C, 3 h under gentle flow of Ar. In each cycle, 0.5 mL FA is added. The solution is stirred overnight at 90 °C between finishing a cycle and commencing the next. In the fourth cycle 1 mL FA added after leaving the solution of the catalyst in IL stirring overnight at 90 °C.

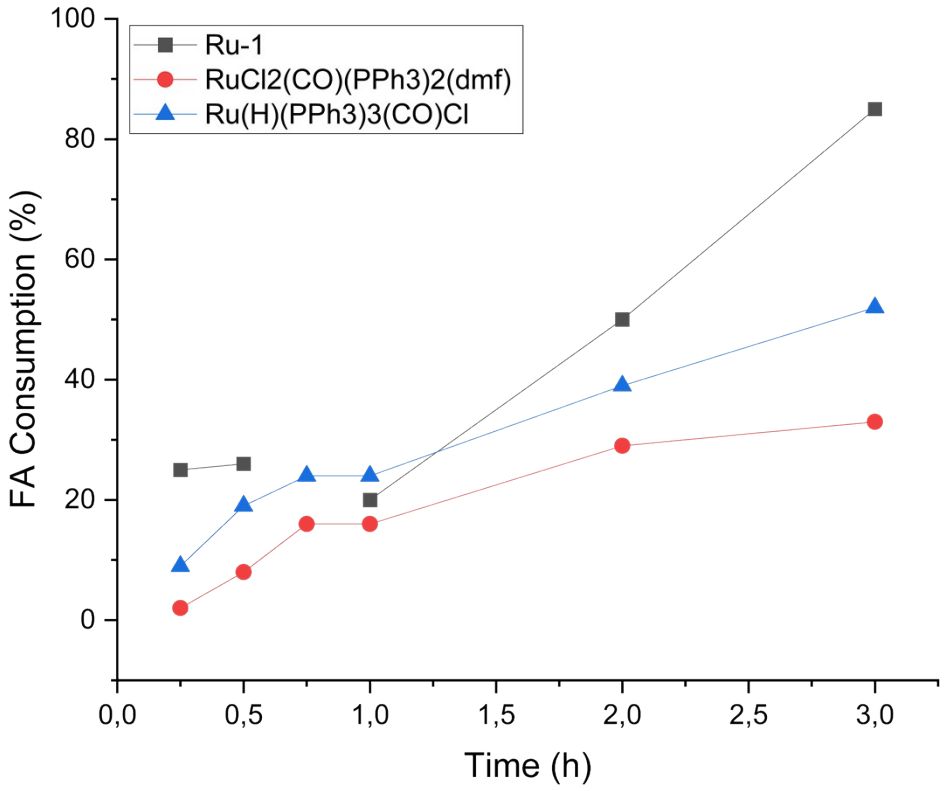

Figure S29. FADH fourth cycle, after adding an excess of FA (1 mL). Comparison among the complexes tested.

[a]Standard reaction conditions: **Ru catalyst** (0.1 mol% in first cycle), EMIM $PO_2(OEt)_2$ (1 mL), FA (0.5 or 1.0 mL), 90 °C, 3 h under gentle flow of Ar. In each cycle, 0.5 mL FA is added. The solution is stirred overnight at 90 °C between finishing a cycle and commencing the next. In the fourth cycle 1 mL FA added after leaving the solution of the catalyst in IL stirring overnight at 90 °C.

Bibliography

(1) Morales-Morales D. *et al.* in High yield carbonylation of $[RuCl_2(PPh_3)_3]$ using dimethylformamide (DMF) as convenient source of CO. The X-ray crystal structure of $[RuCl_2(CO)(DMF)(PPh_3)_2]$. *J. Mol. Struct*., **689**, 137-141 (2004)

(2) Fulmer, G. R. *et al.* in NMR chemical shifts of trace impurities: Common laboratory solvents, organics, and gases in deuterated solvents relevant to the organometallic chemist. *Organometallics* **29**, 2176–2179 (2010).

(3) Puschmann H. *et al.* in OLEX2: a complete structure solution, refinement and analysis program, *J. Appl. Crystallogr*. **42**, 339–341 (2009)

(4) G.M. Sheldrick in SHELXT – Integrated space-group and crystal-structure determination, *Acta Crystallogr. Sect. A Found. Adv*. **71**, 3–8 (2015).

(5) R. Zhong, Z. Wei, W. Zhang, S. Liu and Q. Liu, *Chem*, 2019, **5**, 1552–1566.

(6) J. Houghton, G. Dyson, R. E. Douthwaite, A. C. Whitwood and B. M. Kariuki, *Dalton Trans.*, 2007, 3065–3073.

(7) C.-F. Yang, T. Lu, X.-T. Chen and Z.-L. Xue, *Chem. Commun.*, 2018, **54**, 7830–7833.

(8) W. B. Cross, C. G. Daly, R. L. Ackerman, I. R. George and K. Singh, *Dalton Trans.*, 2011, **40**, 495–505.

(9) W. Wei, Y. Qin, M. Luo, P. Xia and M. S. Wong, *Organometallics*, 2008, **27**, 2268–2272.